

1 Unambiguous evidence of old soil carbon in grass biosilica particles

2

3 Paul E. Reyerson^{1,2, †}, Anne Alexandre³, Araks Harutyunyan¹, Remi Corbineau³, Hector A.
4 Martinez De La Torre¹, Franz Badeck⁴, Luigi Cattivelli⁴, Guaciara M. Santos^{1,*}

5

6 ¹Earth System Science, University of California, Irvine, USA.

7 ²Department of Botany, University of Wisconsin-Madison, USA.

8 ³Aix Marseille Université, CNRS, IRD, CEREGE UM34, 13545 Aix-en-Provence Cedex 4,
9 France

10 ⁴Consiglio per la Ricerca in Agricoltura e l'analisi dell'economia agraria - Genomics Research
11 Centre, Fiorenzuola d'Arda, Italy.

12 [†]Current address: Department of Geography and Earth Science, University of Wisconsin-La
13 Crosse, USA.

14

15 Keywords: phytoliths, biomineralization, soil organic matter, root uptake, carbon sequestration

16

17

18 *Corresponding author. Guaciara M. Santos, Department of Earth System Science, 1222 Croul
19 Hall, University of California, Irvine, Irvine, CA, 92697-3100, USA, phone: (+1-949-824-3674),
20 fax: (+1-949-824-3256), E-mail address: gdossant@uci.edu

21 **Abstract**

22 Plant biosilica particles (phytoliths) contain small amounts of carbon called phytC. Based
23 on the assumptions that phytC is of photosynthetic origin and a closed system, claims were
24 recently made that phytoliths from several agriculturally important monocotyledonous species
25 play a significant role in atmospheric CO₂ sequestration. However, anomalous phytC
26 radiocarbon (¹⁴C) dates suggested contributions from a non-photosynthetic source to phytC. Here
27 we address this non-photosynthetic source hypothesis using comparative isotopic measurements
28 (¹⁴C and δ¹³C) of phytC, plant tissues, atmospheric CO₂, and soil organic matter. State-of-the-art
29 methods assured phytolith purity, while sequential stepwise-combustion revealed complex
30 chemical-thermal decomposability properties of phytC. Although photosynthesis is the main
31 source of carbon in plant tissue, it was found that phytC is partially derived from soil carbon that
32 can be several thousand years old. The fact that phytC is not uniquely constituted of
33 photosynthetic C limits the usefulness of phytC either as a dating tool or as a significant sink of
34 atmospheric CO₂. It additionally calls for further experiments to investigate how SOM-derived C
35 is accessible to roots and accumulates in plant biosilica, for a better understanding of the
36 mechanistic processes underlying the silicon biomineralization process in higher plants.

37

38

39 **1. Introduction**

40 Silicon (Si) is the most abundant element in the Earth's crust and is widely recycled by
41 higher plants. Si is acquired by roots from soils and precipitated in or between the cells as
42 micrometric hydrous amorphous biosilica particles called phytoliths. Phytolith abundances range
43 from <1% of dry weight (d.wt) in many plants to several % d.wt in grasses that are Si-
44 accumulators (Geis, 1973, Runge, 1999, Webb and Longstaffe, 2000; Raven, 2003). Phytoliths
45 contain small amounts of carbon (C) occluded during silica precipitation (Alexandre et al.,
46 2015), commonly termed as phytC or phytOC and assumed to be of photosynthetic origin (Carter
47 2009, Piperno 2006) (Figure 1a). Thus, phytC isotopic signatures ($\delta^{13}\text{C}$ and ^{14}C) obtained from
48 buried soils and sedimentary archives have been interpreted in terms of paleoenvironmental
49 changes (Kelly et al., 1991, Carter, 2009; McInerney et al., 2011), or used as a dating tool
50 (McClaran and Umlauf, 2000; Piperno and Stothert, 2003; Parr and Sullivan, 2005, Piperno,
51 2006).

52 Motivated by anthropogenic emissions of carbon dioxide (CO_2) (Mauna Loa
53 Observatory; NOAA-ESRL data at <http://www.esrl.noaa.gov/>) and their direct association with
54 climate change, a set of recent studies has advanced the idea that many monocotyledonous crop
55 species (bamboo, sugarcane, maize, rice, etc.) as well as grasslands in general (among the largest
56 ecosystems in the world - Suttie et al., 2005) may play a significant role in C sequestration
57 through a newly evidenced mechanism: CO_2 biosequestration in grass biosilica particles (Parr
58 and Sullivan, 2011, Parr et al., 2010, Parr et al., 2009, Parr and Sullivan, 2005, Song et al., 2013,
59 Song et al., 2014, Toma et al., 2013). If correct, encapsulated atmospheric CO_2 can be slowly
60 and steadily accumulated in soils, with turnover times on the order of several hundreds to
61 thousands of years (Parr and Sullivan, 2005). Selective use of silica accumulator crops could
62 further enhance this sequestration mechanism (Song et al., 2013).

63 However, the validity of these interpretations has recently been challenged. First,
64 attempts to properly calibrate the geochemical signals borne by phytC were inconclusive
65 (Wilding, 1967, Kelly et al., 1991, McClaran and Umlauf, 2000, Smith and White, 2004, Webb
66 and Longstaffe, 2010). Second, differences in the efficiency of phytolith extraction protocols
67 may have contributed to inconsistencies and overestimations in phytC quantification (from 0.1 to
68 20% of phytolith d.wt.) (Corbineau et al., 2013 and references therein, Song et al. 2014 and
69 references therein). Third, systematic offsets of phytC ^{14}C ages relative to the ^{14}C ages of the

70 plant tissues from which phytoliths originate have been published (Santos et al. 2010, Santos et
71 al. 2012a,b, Sullivan and Parr 2013, Yin et al. 2014, Piperno 2015, Santos et al. 2016). These
72 offsets can be as large as hundreds to several thousands of years, regardless of the chemical
73 protocol used for phytolith extractions, indicating the presence of a secondary contributor of C to
74 phytC. Together, these observations led to the hypothesis that a whole or a fraction of phytC may
75 come from old soil C (Santos et al., 2012a) (Figure 1b). Previous analyses of macromolecules
76 embedded in phytoliths suggested a variety of organic molecules (Bauer et al., 2011 and
77 references therein), but there is no direct evidence that they are solely synthesized by the plant.
78 Moreover, a recent Nano Secondary Ion Mass Spectrometry (NanoSIMS) investigation of phytC
79 distribution in the silica structure suggests that a significant part of phytC can be lost at the very
80 first stage of phytolith dissolution (Alexandre et al., 2015), thus dissociating the concept of
81 phytC protection from phytolith stability.

82 Therefore, if the soil C to phytC hypothesis is definitively confirmed, it casts doubt on
83 the efficiency of paleoenvironmental reconstructions based on phytC as a proxy of plant C, and
84 raises questions regarding the present estimates of crop and grasslands phytolith efficiency in
85 sequestering atmospheric CO₂, as well as its assessment of long-term stabilization in soils based
86 on fossil phytolith ¹⁴C dating (decades versus hundreds, or thousands of years, as suggested by
87 Parr and Sullivan, 2005). Additionally, confirmation of a dual origin (soil organic matter (SOM)
88 and photosynthetic) of phytC would open new questions regarding plant-soil interactions and
89 SOM recycling, relevant for our understanding of the role of terrestrial ecosystems in the C
90 cycle.

91 To unequivocally establish that a fraction of phytC is indeed from soils, a robust dataset
92 is produced here by considering and ruling out all other factors that can possibly bias the isotopic
93 signatures of phytC. We reassess the old soil C contribution to phytC hypothesis (Santos et al.
94 2012a) on the basis of >200 isotopic results ($\delta^{13}\text{C}$ and/or ¹⁴C) of phytoliths and associated
95 materials (grass tissues, SOM fractions, amendments and hydroponic solutions, CO₂ respired
96 from substrates or extracted from air). Pure phytolith concentrates were acquired from sets of
97 above and below-ground C manipulation experiments. Phytolith concentrates were extracted
98 using several protocols with different degrees of aggressiveness (Corbineau et al. 2013) in four
99 different laboratories. Cutting-edge techniques assured phytolith purity, and multiple analyses of
100 carbon isotope reference materials assured high quality and reproducibility of the isotopic

101 results. Furthermore, to establish a link between phytC heterogeneity in the sense of molecular
102 complexity and resistance to oxidation (labile vs. recalcitrant), we subjected duplicates of pure
103 phytolith extracts to thermal treatments. The multi-methodology approach used in this study
104 allows us to completely address: a) the anomalous ^{14}C results associated with phytC in the
105 literature, b) the implications of a soil C contribution to phytC for ^{14}C geochronology dates, and
106 c) the shortcomings of using phytC as an atmospheric CO_2 sink.

107

108 **2. Material and Methods**

109 **2.1. Samples**

110 Our experimental design is based on a two-step process. First, in order to evidence
111 whether the ^{14}C signatures of phytC are solely of photosynthetic origin, we select samples from
112 known-year specimens, and compare plant material grown under normal atmospheric CO_2
113 conditions to the artificially altered plant C isotope content of photosynthetically assimilated
114 depleted- $^{14}\text{CO}_2$ from Free Air Carbon Enrichment (FACE) experiments (section 2.1.1). Second,
115 we seek to establish a causal connection between soil C and phytC by selecting samples from
116 plant material grown under normal atmospheric CO_2 conditions, but altered substrate carbon
117 pools (section 2.1.2). In both cases phytC and an array of samples associated with it were
118 selected.

119

120 **2.1.1. Above ground C manipulation experiments**

121 The FACE experiments exposed the plants to elevated atmospheric CO_2 concentrations
122 by continuously releasing CO_2 through jets from tubes installed in the surroundings and within
123 the enclosures of the cultivation plots. Target mixing ratios of atmospheric and geologic CO_2
124 were maintained on plots until leaves were senescent and/or ready for harvesting.

125 Two grass species (*Sorghum bicolor* and *Triticum durum*) were grown in two FACE
126 experiments, respectively: at the Maricopa Agricultural Center (University of Arizona, USA) in
127 1998-1999 (Ottman et al., 2001), and at the Genomics Research Centre of CREA (Consiglio per
128 la ricerca in agricoltura e l'analisi dell'economia agraria) in Fiorenzuola d'Arda, Italy, in 2011-
129 2012 (Badeck et al., 2012 - <http://centrodigenomica.entecra.it/research/durumFACE>). For each
130 experiment, a plot cultivated under ambient atmospheric CO_2 was compared to a plot cultivated

131 under atmosphere enriched by 160-200ppm in fossil hydrothermal CO₂, and therefore free of ¹⁴C
132 (Leavitt, 1994, Ottman et al., 2001, Badeck et al., 2012). In terms of stable isotopic labelling, at
133 the sorghum site the enriched CO₂ had a δ¹³C value of -40‰ from 1995 to 1998. This stronger
134 isotopic label was obtained from a mixture of natural CO₂ from the Springerville, Arizona, USA
135 geologic wells with 15% petroleum-derived CO₂. During 1998-1999 only fossil hydrothermal
136 CO₂ was used (δ¹³C = -4.36 ‰), while the background air δ¹³C was -8‰ (Leavitt et al., 2001).
137 At the durum wheat site, the commercial fossil CO₂ from the Rapolano Terme, Poggio S. Cecilia
138 (Tuscany) well had a δ¹³C of -6.07‰, which was slightly positive compared to the ambient CO₂
139 value of -8‰.

140 Two samples of mixed stems and leaves (~100 g) were obtained from the sorghum site,
141 while four separated samples (300-400 g each) of stems and leaves were collected at the durum
142 wheat site. Eight soil samples (~5 g each) collected from the furrows of the sorghum plots at
143 depths of 0-15, 15-30, 30-45 and 45-60 cm were also obtained from the archives of the
144 Laboratory of Tree-Ring Research, University of Arizona, USA. While two soil samples were
145 collected from the ongoing durum wheat experimental plots at a depth of 0-15 cm (~15 g each)
146 during plant biomass harvesting.

147 To determine the precise ¹⁴C activity of the plant materials, radiocarbon measurements
148 were conducted before the phytolith extractions started. Since the commercial CO₂ used in both
149 FACE enrichment sites was from a fossil source, its ¹⁴C signature as fraction of modern carbon
150 (FmC or Fm¹⁴C; Stuiver and Polach, 1977) was close to zero. Therefore, the ¹⁴C signature of the
151 enriched CO₂ was highly depleted compared to ambient air, and the plant tissues were tagged
152 accordingly. Radiocarbon signatures of the plant tissue yielded Fm¹⁴C values of 0.640 (~3.6 kyrs
153 BP; ¹⁴C years before present or 1950; UCIAMS53273 and 53274; Table S1 in Supplement) and
154 0.556 (~4.7 kyrs BP; UCIAMS109000 and 109001; Table S2 in Supplement) at the sorghum and
155 durum sites, respectively. Alternatively, plant tissue from ambient CO₂ plots was expected to
156 yield the prescribed atmospheric ¹⁴CO₂ values of the given year that the growing season took
157 place. At the sorghum site, the Fm¹⁴C value of the bulk biomass harvested at the ambient CO₂
158 plot matched with the Fm¹⁴C value of the CO₂ of the year of harvest (e.g. Fm¹⁴C ≈ 1.097,
159 equivalent to the atmospheric ¹⁴CO₂ signature measured from clean air in 1999 -
160 <http://calib.qub.ac.uk/CALIBomb/> database and calibration software). This ¹⁴C signature is
161 higher than the present-day ambient CO₂ due to nuclear weapon tests carried out during the

162 1950s and 1960s (Levin, 1997, Levin et al., 2013). The nuclear weapon tests doubled the ^{14}C
163 content in the atmosphere, which created an isotopic chronometer (the ^{14}C bomb peak) during
164 the last 60 years for all living organisms. At the durum wheat site, however, the ^{14}C signature of
165 the biomass harvested at the ambient CO_2 plot was slightly depleted ($\text{Fm}^{14}\text{C} \approx 1.017$), as
166 expected for CO_2 above urban areas in Europe in the early 2010s. For comparison, the ^{14}C
167 signature of atmospheric-clean CO_2 stations in Central Europe was $\text{Fm}^{14}\text{C} = 1.040$ in 2012
168 (Levin, 1997, Levin et al., 2013).

169

170 **2.1.2. Below ground C manipulation experiment**

171 The second experiment relies on the simultaneous response of phytC to different carbon
172 amendment treatments of grasses grown under photosynthetic natural conditions (i.e., ambient
173 CO_2 air). *Sorghum bicolor* plants were grown outdoors in a ventilated area at the University of
174 California, Irvine (UCI, USA), in six well-drained 40 L planters (A, B, C, D, E and F) filled with
175 mineral substrates. Five of the planters were enriched with organic nutrients characterized by a
176 broad range of ^{14}C signatures (from bomb spiked to fossil - Tables 1 and 2), while the last
177 contained an inorganic nutrient devoid of C as a control (planter F). Although much concerning
178 the direct root absorption of natural carbon remains unknown, beneficial responses of root and
179 plant growth have been reported in association with the addition of either inorganic carbon
180 (Hibberd and Quick, 2002) and/or humic acids (Nardi et al., 2002). Consequently, we chose as
181 substrate for Planter B, a natural carbonate-based sedimentary deposit mixed with organic carbon
182 detritus of equal/even-age. For Planter E, fossil humic acids (extracted from leonardite) were
183 chosen as the OC source.

184 Plants were fed as needed solely with 2 L of ultra-pure water (Planter A), or with a
185 combination of ultra-pure water and their respective fertilizers and SiO_2 providers (Planters B-F)
186 at a concentration of 1% (v/v) (Table 2). Additionally, the CO_2 in the air surrounding the planters
187 was isotopically monitored by collecting air in evacuated 6 L cylinders for the duration of the
188 experiment with the purpose of characterizing the local atmospheric CO_2 close to planters, and to
189 serve as a reference for the ^{14}C signatures expected from plant tissue organs. Also, we
190 isotopically measured commercial (sorghum) seeds to check if their ^{14}C signatures were recent.
191 Finally, CO_2 fluxes respired from the planter substrates were also sampled to evaluate their

192 putative contribution to the phytC ^{14}C signature. After 3.5 months the *Sorghum bicolor* plants
193 (stem and leaf) were harvested in preparation for phytolith extractions and isotopic analyses.

194

195 **2.2. Laboratory Procedures**

196 **2.2.1. Plant treatment and phytolith extraction**

197 Stems and leaves samples (50-100 g each) were thoroughly rinsed with warm ultrapure
198 water to remove air-dust, dried at 60 °C and ground using an industrial mill (IKA[®] M20
199 Universal Mill). About 10 mg of each sample was kept for bulk tissue ^{14}C and $\delta^{13}\text{C}$ analyses.

200 Four phytolith extraction protocols with increasing aggressiveness (via organic
201 compound oxidation and silica dissolution) were used to treat the samples from the above ground
202 C manipulation experiment (Fig. 2). The protocols have been previously described in detail by
203 Corbineau et al. (2013). They are based either on acid digestion and alkali or on multi-step dry
204 ashing and acid digestion. They are summarized below and in Figure 2.

- 205 i. *Protocols 1a and 1b* - Plant samples were subject to strong wet-digestion steps in
206 order to oxidize the organic matter (e.g., 1N HCl/2 hours, hot H_2SO_4 /24 hours plus
207 30% H_2O_2 for 2-3 days, and > 65% HNO_3 plus 1 g KClO_3 for 24 hours). This was
208 followed by 30 min of immersion in KOH solution at pH11 (protocol 1a) or pH13
209 (protocol 1b). The KOH immersions allowed final removal of any alkali-soluble
210 forms of organic compounds remaining on phytolith surfaces.
- 211 ii. *Protocols 2a and 2b* - Plant samples were subjected to dry-ashing. Stepwise increases
212 in temperature were used from 300°C to 500°C and the samples were then kept at
213 500°C for 6 hours (protocol 2a) or 12 hours (protocol 2b). Samples were then
214 digested in a >65% HNO_3 and 70% HClO_4 mixture (2:1).

215

216 In order to assess local ^{14}C contamination during chemical extractions, four laboratories
217 were involved in the extractions. They are UCI (USA), French National Centre for Scientific
218 Research (CEREGE, France), the Soils and Sediments Analysis Lab (SSAL, the University of
219 Wisconsin-Madison, USA), and the National Lacustrine Core Facility (LacCore, the University
220 of Minnesota, Twin Cities, USA). Aliquots of pre-baked (900°C/3 hours) silicon dioxide powder
221 (SiO_2 ; mesh# -325, Sigma Aldrich, St. Louis, MO, USA) were chemically pre-treated in parallel

222 with the plant samples, and later analyzed as phytolith extract to provide independent blank data
223 for each laboratory following the procedures described in Santos et al. (2010).

224 Due to the limited amount of plant biomass produced by the below ground C
225 manipulation experiment (session 2.1.2), only two protocols were tested (1a and 2b) at only three
226 of the laboratories (UCI, CEREGE and LacCore), followed by blank sample materials as
227 required.

228

229 **2.2.2. Soil extraction fractions**

230 Soils from the above ground C manipulation experiment were physically cleaned of roots
231 and stones. The bulk SOM fraction was isolated after carbonate removal in 1N HCl baths at 60
232 °C. The refractory (alkali-insoluble) fraction was further isolated via multiple baths in 1M NaOH
233 at 60 °C, followed by 1N HCl rinses (Santos and Ormsby, 2013). Upon chemical treatment,
234 samples were adjusted to pH neutral and dried in a vacuum oven (Savant RT 100A refrigerated
235 vapor vacuum pump system).

236 Amendments from the below ground C experiment were not subject to any chemical
237 pretreatment, except for the tests performed to small aliquots of greensand (GS, Table 1),
238 allowing us to isolate the organic fraction from its bulk mixture.

239

240 **2.2.3. CO₂ flux measurements**

241 In the frame of the below ground C manipulation experiment, the rate of CO₂ respired
242 from *Sorghum bicolor* foliage (after sprouting), root systems and substrate was measured using
243 closed dynamic soil CO₂ flux chambers (Czimzik et al., 2006). Chamber headspace gasses were
244 circulated through an infrared gas analyzer (840, 1400, LI-COR, Lincoln, NE, USA,) for 6
245 minutes at 0.5 L per minute, and the CO₂ concentration was recorded every second. Once
246 headspace CO₂ concentrations reached twice that of ambient-air, the CO₂ was collected in a
247 molecular sieve trap for isotopic analysis, followed by ambient-air samples to serve as
248 references.

249

250 **2.3. Analytical procedures**

251 **2.3.1. Phytolith concentrate purity analysis**

252 Small particulate organic contamination of phytolith concentrates may considerably
253 bias isotopic and quantitative analyses of phytC. The purity of the phytolith concentrates was
254 thus verified by Scanning Electron Microscopy with Energy-dispersive X-ray spectroscopy
255 (SEM-EDS) (Corbineau et al., 2013). Extracted phytoliths, mounted directly on pre-cleaned
256 aluminum stubs, were analyzed with a Schottky Thermal Field Emission FEI/Philips XL-30
257 SEM with back-scattering electron detector. EDS semi-quantitative analyses of C and Si were
258 obtained from 10 to 30 μm locations on selected particles. Special attention was paid to organic-
259 like particles showing tissue-like or non-phytolith morphologies. A total of ~ 30 analyses per
260 sample were made. Samples with all C:Si peaks area ratios < 0.1 were reported as devoid of
261 organic particles. The equal/even accuracy and precision of the EDS analyses were evaluated by
262 multiple measurements [Mean value (M)= 1.17 ; Standard Deviation (SD)= 0.02 ; $n=21$] of a
263 silicon carbide (SiC) standard (#9441, Micro-Analyses Consultant Instrument LTD, St. Ives,
264 UK).

265

266 **2.3.2. Stable Isotope Analysis**

267 Stems/leaves, SOM fractions, nutrients/fertilizers and phytolith samples were analyzed
268 for their total C content and stable C isotope ratio ($\delta^{13}\text{C}$) using a continuous flow stable isotope
269 ratio mass spectrometer (Delta-Plus CFIRMS) interfaced with a Fisons NA-1500NC (for solid
270 materials) and a Gasbench II (for CO_2 input).

271 About 10 mg of phytoliths and 25 mg of soil were weighed out into pre-baked (100°C
272 per 2 hours) tin capsules (5 x 9 mm capsules from Costech Analytical Technologies Inc.,
273 Valencia, CA, USA) using a pre-calibrated microbalance (Sartorius AG, Göttingen, Germany).
274 For accurate integration and calibration of carbon peaks of phytolith samples ($\sim 0.1\%$ C),
275 measurements were obtained by decreasing the helium carrier flow rate, and by measuring
276 several size-matched aliquots of standards from the National Institute of Standards Technology.
277 Aliquots of SiO_2 blanks and fossil phytoliths (MSG70) used as an internal standard at CEREGE
278 (Alexandre et al., 2015, Crespin et al., 2008) were included for background corrections and
279 accuracy (Santos et al., 2010), respectively. For the bulk tissue samples, aliquots of CO_2 gas
280 were recovered after combustion, and sent to CFIRMS, which has a typical precision of 0.1%.
281 Stable isotope results are reported as δ values in ‰ relative to the Vienna Pee Dee Belemnite
282 (vPDB).

283

284 **2.3.3. Radiocarbon Analysis**

285 Stems/leaves, SOM fractions, nutrients/fertilizers, CO₂ and phytolith samples were
286 processed for ¹⁴C accelerator mass spectrometry (AMS) analyses. About 2 mg of plant tissue, 20-
287 100 mg of SOM and 15-300 mg of phytoliths were loaded for tube-sealed combustion (Santos et
288 al., 2004). To avoid CO₂ adsorption on phytolith surfaces, the loaded samples were kept and
289 transferred warm (at 160 °C) to the evacuated line for sealing (Santos et al., 2010). Liquid
290 solutions were freeze-dried directly into tubes prior to combustion. Atmospheric CO₂ was
291 extracted from 6 L collection flasks of whole air, by attaching the flasks to an evacuated line. A
292 similar procedure was used to recover the CO₂ collected in molecular sieve traps (from flux
293 chambers). Once the CO₂ was cryogenically separated from other gasses, it was then transferred
294 to a Pyrex tube at a flame-off port and sealed (Santos et al., 2010). Samples of CO₂ from tube-
295 sealed combustions, flasks and traps were cryogenically isolated, and reduced to graphite (Santos
296 et al., 2007, Xu et al., 2007), or transferred to Gasbench II CFIRMS for isotopic analysis.

297 The ¹⁴C measurements were performed at the Keck-CCAMS Facility (UCI). Precision
298 and accuracy in measurements on >0.7 mg of near-modern carbon samples are typically 0.2–
299 0.3% (Beverly et al., 2010), and 1% on samples in the 0.01 mgC range (Santos et al., 2007). The
300 instrument provides the isotopic ratio ¹³C/¹²C, allowing for fractionation effects (either
301 spectrometer induced or arising from biochemical processes) to be corrected for all targets
302 measured.

303 Blanks from SiO₂ aliquots were also measured to provide background corrections. All
304 labs and extraction protocols showed similar procedural blanks (~0.003 mg of modern C and
305 ~0.002 mg of ¹⁴C free^a. Those values were subtracted from the ¹⁴C data, including the results
306 obtained from the MSG70 reference material, for accuracy. Details on such background
307 subtractions can be found elsewhere (Santos et al., 2010). Radiocarbon results were expressed as
308 Fm¹⁴C and when appropriate were discussed as ages.

^a The term ¹⁴C free is used in association with materials from which the original ¹⁴C radioisotope content has been reduced to zero or close to zero. However, those materials obviously continue to maintain their stable amounts of ¹²C and ¹³C. Consequently, the addition of ¹⁴C free (or organic carbon from subfossil ¹⁴C signatures) to pools of C containing present-day atmospheric CO₂ signals will lower the overall ¹⁴C signature of the pool. For each 1% fossil C present, an offset of 80 years is expected (Santos et al. 2016).

309

310 **2.3.4. Thermal Analysis**

311 We performed thermal analysis of phytoliths on a modified Thermal-Optical Carbon
312 Aerosol Analyzer (RT 3080, Sunset Laboratory Inc.) (Bae et al., 2004). Phytolith concentrates of
313 7-10 mg were loaded onto a customized spoon (Jelight Company, Inc. USA), placed into the
314 instrument and kept at 50 °C for ~10 minutes for surface cleansing. The stepwise temperature
315 ramp started at 50 °C and ended at 850 °C 50 minutes later. Pure oxygen (65 mL/min) was used
316 to avoid refractory carbon (char) formation. The CO₂ evolved was injected into a manganese
317 dioxide oven at 870 °C, and later quantified by a non-dispersive infrared detector. Typical multi-
318 point calibration curves, when analyzing known quantities of C ranging from 2-120 µg, yielded
319 correlation coefficients greater than 0.998.

320 Two phytolith samples were analyzed. Durum wheat leaf phytoliths extracted using
321 protocol 1a, and the CEREGE internal standard, MSG70, made of highly weathered fossil
322 phytoliths (Alexandre et al., 2015, Crespin et al., 2008).

323

324 **3. Results and Discussions**

325 **3.1. Isotopic results from above-ground C manipulation experiments**

326 A total of 21 individual phytolith concentrates were produced for the above-ground
327 experiments by all laboratories involved in this project Those samples are tabulated in the
328 Supplement (Tables S1 and S2), followed by details on the sample processing (protocols,
329 laboratory and measurement identifiers). Note that when sufficient plant material was available
330 (which was the case for the durum wheat samples) some labs could replicate the extraction (i.e.
331 processing the same pool of biomass following the same protocol).

332 From those 21 phytolith concentrates, 51 ¹⁴C results were produced to determine the
333 phytC ¹⁴C signatures (number of targets includes duplicates and/or replicates, as specified in
334 Tables S1 and S2). Two phytC ¹⁴C targets from MSG70, a fossil phytolith internal standard at
335 CEREGE, were also produced to evaluate measurement reproducibility. Overall, the precision
336 and accuracy of the phytC ¹⁴C data were better than 0.3%, based on duplicates and triplicates of
337 graphite samples > 0.5 mgC. For the smaller sized samples, 1% or better were recorded in most
338 cases, even after background corrections based on measurements of multiple SiO₂ aliquots were
339 propagated into individual uncertainties (Tables S1 and S2). We have not identified significant

340 differences in inter-laboratory analyses when using the same protocol on subsamples of the same
341 biomass sample, and/or when evaluating procedural blank materials (added to every batch
342 analyzed – details in section 2.3.3). To help with determining the phytC carbon sources, other
343 ¹⁴C results shown in tables S1 and S2 are from the stems/leaves and SOM fractions (e.g. the
344 carbon pools associated with the labile-accessible and recalcitrant (alkali-insoluble).

345 PhytC concentrations were consistent for a given extraction method but showed a clear
346 decreasing trend with increasing protocol aggressiveness. The phytC yields (phytC % relative to
347 the d.wt of phytoliths) averages ranged from 0.24 to 0.06% for the less aggressive protocols 1a
348 and 1b and from 0.05 and 0.002% for the more aggressive protocols 2a and 2b (Figure 2a, and
349 Tables S1, S2).

350 Phytoliths extracted from either sorghum or durum wheat using protocol 1a produced
351 phytC ¹⁴C signatures closest to the values of the stems and leaves of origin regardless of air CO₂
352 concentration (ambient vs enriched CO₂) and grass species (Figure 2b). However, phytC ¹⁴C
353 offsets were still evident when compared to the expected values given the year of harvest or
354 artificial tagging (Table S1). For sorghum, absolute offsets varied from 85 (UCIAMS123579 and
355 123580) to 610 years (UCIAMS123577 and 123578) when using protocol 1a. The maximum
356 offset increased when using protocols 1b (2633 years; UCIAMS95338), 2a (1920 years;
357 UCIAMS130339), and 2b (1990 ¹⁴C years; UCIAMS95335 to 95337). Durum wheat ambient
358 phytC ¹⁴C absolute offsets varied from 105 (UCIAMS123572) to 1925 years (UCIAMS125986),
359 while phytC offsets from enriched plots varied from 310 (UCIAMS123570 and 123571) to 2885
360 years (UCIAMS125983).

361 The hypothesis that there is a contribution of SOM-derived C to phytC was tested
362 estimating phytC as a mixture of i) C derived from plant photosynthesis and ii) C derived from
363 the oldest SOM fraction measured. The mixing equation (eq.1) is:

364

$$365 \text{ Oldest SOM-derived C contribution} = (\text{Fm}^{14}\text{C}_{\text{SOM}} - \text{Fm}^{14}\text{C}_{\text{SL}}) / (\text{Fm}^{14}\text{C}_{\text{phytC}} - \text{Fm}^{14}\text{C}_{\text{SL}}) \quad (\text{eq. 1})$$

366

367 where the ¹⁴C signatures of the oldest SOM, stems and leaves (SL) and phytC are expressed as
368 $\text{Fm}^{14}\text{C}_{\text{SOM}}$, $\text{Fm}^{14}\text{C}_{\text{SL}}$ and $\text{Fm}^{14}\text{C}_{\text{phytC}}$. $\text{Fm}^{14}\text{C}_{\text{phytC}}$ was expressed relative to $\text{Fm}^{14}\text{C}_{\text{SOM}}$ (assigned a
369 contribution value of 1) and $\text{Fm}^{14}\text{C}_{\text{SL}}$ (assigned a contribution value of 0). The average Fm^{14}C
370 value of the oldest SOM-C fractions measured in each experiment (i.e., the Fm^{14}C average value

371 of the SOM 45-60 cm fraction for *S. bicolor* plots – Table S1 in Supplement, and the refractory
372 0-15 cm fraction for *T. durum* plots – Table S2 in Supplement) were used for $Fm^{14}C_{SOM}$.

373 The mixing curves associated with the SOM-derived C to phytC hypothesis are presented
374 in figure 2b. The $Fm^{14}C$ values of two phytC samples from the Sorghum Ambient CO_2
375 experiment obtained using protocol 1a (UCIAMS123579 and 123580) and one phytC sample
376 from the Durum wheat Enriched CO_2 experiment obtained using protocol 1b (UCIAMS130339)
377 were higher than $Fm^{14}C$ values of the stems and leaves of origin, indicating that the soil pool still
378 has remnants of ^{14}C -labeled OC from the 1950s thermonuclear tests (Levin, 1997, Levin et al.
379 2013). In this case the SOM-derived C was assigned a contribution value of 0, and the stems and
380 leaves a contribution value of 1 in figure 2b. Conversely, some of the phytC $Fm^{14}C$ values from
381 the Durum wheat Enriched CO_2 experiment, obtained using protocols 1a, 2a and 2b
382 (UCIAMS123566, 123567, 125985, 130334 and 130335), were lower (^{14}C age older) than the
383 $Fm^{14}C$ value of the oldest SOM fraction or 1 in figure 2b. This pattern suggests that the so-called
384 oldest SOM fraction, which is a mixture of old and young SOM (Schrumpf et al., 2013) may still
385 be “younger” than present-day in terms of its ^{14}C signatures, if the C pool is still bearing some
386 bomb-produced ^{14}C OM or much older if aromatic complexes are dominant (Teller et al. 2003,
387 Torn et al. 2009). For the sorghum experiment this trend was particularly obvious, as the ambient
388 CO_2 and the upper soil layers were clearly imprinted with bomb ^{14}C (Levin, 1997). Therefore,
389 figure 2b clearly showed that the phytC $Fm^{14}C$ values unambiguously trend toward the $Fm^{14}C$
390 value (or ^{14}C age) of the oldest SOM fraction. Overall, the crucial point to be noticed is that the
391 phytC ^{14}C offsets shifted linearly towards negative values if the oldest SOM fraction was older
392 than the biomass of origin (Sorghum Ambient and Durum wheat Ambient, Figure 2a), and
393 towards positive values when the oldest SOM fraction was younger (Sorghum Enriched, Figure
394 2a). Thus, phytC ^{14}C differences were clearly linked to the oldest SOM ^{14}C ages. Moreover, the
395 agreement in phytC ^{14}C values obtained from stems and leaves indicated that the offsets were not
396 linked to plant anatomy.

397 Regarding $\delta^{13}C$ values, the phytC offsets relative to the tissue of origin did not
398 systematically trend towards SOM $\delta^{13}C$ values, except for the Sorghum Ambient phytC
399 undergoing the 2b protocol ($-21.6 \pm 0.1\text{‰}$ ($n=2$)) as indicated in Figure 3; UCIAMS95335 and
400 95336). As described earlier, this protocol tends to isolate the most recalcitrant phytC fraction.
401 The difference between phytC $\delta^{13}C$ values of durum wheat and sorghum was higher ($\sim 15.7\text{‰}$)

402 than the difference between $\delta^{13}\text{C}$ values of the stems and leaves of origin (e.g. ~ 5.6 vs $\sim 7.2\text{‰}$ for
403 wheat and sorghum, respectively), as previously reported for grasses with C_3 and C_4
404 photosynthetic pathways (Webb and Longstaffe, 2000, Webb and Longstaffe, 2010). Without
405 further discrimination of the molecular composition of SOM-derived C absorbed by the plant
406 roots, in-depth discussion of the $\delta^{13}\text{C}$ differences between phytC and plant biomass is difficult.
407 Nevertheless, the observed differences between phytC and stems and leaves $\delta^{13}\text{C}$ values were
408 consistent with previous calibration studies, and were explained by preferential occlusions of
409 plant molecular ^{13}C -depleted compounds in phytoliths (Webb and Longstaffe, 2010).

410

411 **3.2. Isotopic results from below-ground C manipulation experiments**

412 A total of 12 individual phytolith concentrates and phytC ^{14}C targets were produced for
413 the below-ground experiments, two of those from the same biomass samples (from Planters A
414 and C), but subjected to different degrees of oxidation (e.g. protocols 2a and 2b). Other ^{14}C
415 results shown are from the stems/leaves, nutrients/fertilizers, and CO_2 extracted from 6 L flasks
416 and flux chambers (Figure 4). The complete set of isotopic results and sample processing details
417 are tabulated in the Supplement (Tables S3).

418 Phytoliths produced phytC yields ranging from 0.08 to 0.1% d.wt. when using the less
419 aggressive protocol 1a and from 0.01 to 0.04% d.wt when using the more aggressive protocol 2b
420 (Table S3).

421 Significant offsets of the phytC ^{14}C values relative to the stem and leaf Fm^{14}C values
422 were again found in association with the carbon sources in the soils (e.g.
423 substrates/amendments). The highest phytC ^{14}C offset of 3610 years (UCIAMS104366) was
424 obtained from the phytC ^{14}C from Planter B when using protocol 2b, showing again that the
425 increased age discrepancies were due to protocol aggressiveness (e.g. from 1a to 2b). The effect
426 is also observed in the phytoliths associated with Planter C, which received very low amounts of
427 below-ground organic carbon relative to all other treatments (Tables 1 and 2). Specifically, the
428 Planter C phytC ^{14}C offsets increased from 160 (UCIAMS130346; protocol 1a) to 1150
429 (UCIAMS104362; protocol 2a), and finally to 1760 years (UCIAMS104900; protocol 2b).

430 Even when we processed biomass samples from all Planters following the same protocol
431 (such as the less aggressive 1a protocol), ^{14}C age discrepancies between phytC and the plant of
432 origin were highly evident, and correlated to the ^{14}C signatures of amendments

433 (UCIAMS130344 to 130348). PhytC ^{14}C offsets were greater for amendments containing
434 sufficient amounts of C of extreme ^{14}C -signatures (e.g. positive 320 years to Planter A, and
435 negative 680 years to Planter E in Table S3). Note that the Planter A substrate was composed of
436 rich bulk-complex OC imprinted with ^{14}C -bomb values (or Fm^{14}C signatures higher than
437 present-day values), while the Planter E substrate received a solution of fossil OC ($\text{Fm}^{14}\text{C}=0$;
438 close to ~ 43 kyr BP; $n=3$) (Tables 1 and 2). As in the above C manipulation experiment, in figure
439 4 we assigned values of 0 and 1 to the Fm^{14}C associated with stems and leaves of origin and
440 amendments, respectively (Table S3), and used the same mixing equation (eq.1).

441 The bulk stems and leaves produced Fm^{14}C signatures that were very similar to the local
442 ambient air $^{14}\text{CO}_2$ values collected in the 6L cylinders during the growing season, excluding any
443 possibility that the phytC ^{14}C depletions are a product of urban fossil atmospheric CO_2 fixation.
444 The small discrepancies between the stem and leaf ^{14}C values (e.g. from 25 to 65 years) (Table
445 S3) are attributed to heterogeneities in C distribution within plant cells during C fixation (Pausch
446 and Kuzyakov, 2011, Wichern et al., 2011). The commercial seeds of sorghum were also
447 measured by ^{14}C -AMS (Figure 4) to verify their recent radiocarbon activity (UCIAMS83120 and
448 83121; Table S3). As expected, once early-fixed photosynthetic CO_2 became dominant,
449 remobilized ^{14}C from seeds made little contribution to mature biomass tissue.

450 Although Fm^{14}C values of substrate CO_2 fluxes were depleted towards amendment ^{14}C
451 bulk signatures (UCIAMS83842 to 83845, Table S3), soil CO_2 plant tissue refixation via
452 photosynthesis (and its influence on phytC) was found to be negligible, and cannot be invoked to
453 explain the anomalous phytC ^{14}C results. CO_2 fluxes from the planters' substrates upon sprouting
454 varied from 0.34 to 1.72 ppm/sec ($\approx 10^{-5}$ g/m²/yr) (Table S3), indicating very little microbial
455 activity. For comparison, global soil CO_2 fluxes vary from 60 to 1000 g/m²/yr (Raich and
456 Sclesinger, 1992).

457 $\delta^{13}\text{C}$ offsets between phytC and stems and leaves were $\sim 6.5\text{‰}$ on average, including the
458 phytC from Planter B (which contain a mixed C pool of OM detritus of plant origin and
459 carbonate deposits - Table 1), showing that the inorganic fraction of the soil C was not a
460 significant source of phytC (Figure 5). Also in Figure 5, we show the stable isotopic signatures
461 of the CO_2 fluxes (UCIAMS83842 to 83845; Table S3) collected using closed dynamic soil CO_2
462 flux chambers (Czimzik et al., 2006). The results fell mostly between the air and bulk plant

463 tissue averages, as expected for CO₂ produced from above- and below-ground biomasses,
464 supporting our previous observations of negligible effects of soil CO₂ respired to phytC.

465 This dataset clearly shows that amendment-derived C, adsorbed through root plants,
466 altered the phytC ¹⁴C signatures.

467

468 **3.3. Thermal stability of phytC**

469 Chemical compositional insights on carbonaceous materials can be obtained via oxidation
470 reactivity to thermal treatments; such treatments have been frequently used on organic
471 compounds from soils and sediments (Plante et al. 2011, 2013, Rosenheim et al., 2013). For
472 instance, single bonded carbon structures usually show a lower thermal stability than those
473 dominated by double bonds, such as conjugated and aromatic structures (Harvey et al., 2012).
474 Here, we make use of the same chemical-thermal stability concept to evaluate the heterogeneity
475 of phytC in reacting to heat treatments.

476 Thermograms obtained from phytoliths of the durum wheat leaves and fossil phytoliths
477 (MSG70) indicated a continuum of phytC CO₂ with different degrees of resistance or
478 accessibility (Figure 6). Although the overall production of CO₂ was lower for MSG70, the
479 continuum temperature-dependency pattern of phytC was preserved. For example, at 250 °C
480 both phytolith extracts produced CO₂, however the leaf phytoliths show lesser amounts of CO₂
481 evolved than soil phytoliths. At 500 °C half of the phytC CO₂ in both samples had been evolved,
482 and at 800°C all of the phytC has been completely removed.

483 Phytoliths typically melt at ~573 °C (Deer et al., 1992), but embedded metals (e.g. Al, Fe,
484 etc) within their structures could lead to a decrease in temperature stability (Wu et al., 2014).
485 Nevertheless, phytC that required much higher temperatures (e.g. >> 573° C) to fully oxidize,
486 places it at the upper-end of the carbon recalcitrance continuum (Cheng et al., 2013, Harvey et
487 al., 2012, Plante et al., 2005, 2011, 2013). Furthermore, even if char occurred during combustion
488 leading to some elemental carbon formation, it does not explain the Fm¹⁴C phytC discrepancies
489 obtained here (Figures 2 and 4) or elsewhere (Santos et al., 2010, Santos et al., 2012a, Santos et
490 al., 2012b, Sullivan and Parr, 2013, Yin et al., 2014).

491 Santos et al. (2012a) and Yin et al. (2014) also heated phytolith aliquots from a single
492 extract, and observed shifts in ¹⁴C ages towards older values. This effect is similar to that
493 observed in total carbon or SOM distributions in soils and sediments when subject to thermal

494 decomposability (Plante et al. 2011, 2013). Thus, phytolith extractions that employ heat
495 treatments would better isolate the oldest soil C fraction within phytoliths, as previously found
496 (in sections 3.1. and 3.2). Basically, if the C pool in phytoliths is supposedly homogeneous and
497 from a single source (atmospheric CO₂), the ¹⁴C results from all CO₂ temperature-fractions
498 should be in absolute agreement, as Fernandez et al. (2015) demonstrated by subjecting
499 carbonaceous materials to ramp pyrolysis and subsequently measuring them by ¹⁴C-AMS.

500

501 **4.1. The SOM-derived C to phytC hypothesis set of evidence**

502 Results from both above- and below-ground experiments showed that the ¹⁴C offsets
503 between phytC and stems and leaves pointed toward the oldest SOM ¹⁴C values (Figures 2 and
504 4). This confirmed that a fraction of the old SOM-derived C occluded in phytoliths was more
505 resistant (or less accessible) to oxidation than the occluded C derived from recent photosynthesis
506 or from recent SOM. Once the most labile (or more accessible) C had been removed, the older
507 and more resistant carbon fraction became dominant. This behavior mirrors that in a recent study
508 showing an increase in ¹⁴C age offsets of phytoliths with increasing combustion temperature
509 (Yin et al., 2014), and also the thermal decomposability pattern illustrated in the phytC
510 thermograms (Figure 6).

511 Our findings also imply that a portion of SOM-derived C is absorbed by the roots,
512 transferred to the stems and leaf and finally occluded into phytoliths. In the bulk plant organs,
513 the old SOM-derived C amount is far too small to be ¹⁴C detected in tissue clippings, as it is
514 masked by the large amounts of photosynthetic atmospheric carbon tissue (bulk stems and leaves
515 averaged ~41% carbon; Tables S1-S3). On the other hand, in phytoliths, the old SOM-derived C
516 becomes overrepresented when the most labile-accessible phytC starts to be oxidized. It should
517 be noted that the ¹⁴C ages of the oldest SOM fraction are averaged bulk values that do not yield
518 any precise assessment of the fine-scale ¹⁴C age of the C that may have been absorbed. These
519 drawbacks prevent precise quantification of the old SOM (probably diluted by the young SOM)-
520 derived C contribution to phytC. The impossibility of quantifying precisely the amounts of soil C
521 and associated ¹⁴C signatures in phytC precludes application of any correction that would allow
522 phytC to be used as a reliable dating material. As in any other heterogeneous carbon pool, the
523 phytC continuum can be similarly partitioned differently by distinctive chemical extractions. For
524 instance, in Piperno (2015) the entire dataset of post-bomb Neotropical plant phytolith extracts

525 were neither accurate nor precise. While ^{14}C offsets reached discrepancies as high as 4.4 kyrs
526 between expected calendar ages and phytC, two pairs of phytolith extracts obtained by distinct
527 chemical treatments (sulfuric vs. nitric) yielded a 50 percent reproducibility rate (Table 1, Santos
528 et al. 2016).

529 Recent 3D X-Ray microscopy and NanoSIMS measurements of a phytolith sample from
530 the Durum wheat enriched CO_2 experiment (TD-F-L/1a-CEREGE, Table S1) (Alexandre et al.,
531 2015) suggested two locations for phytC: in micrometric internal cavities and within the silica
532 network. Rapid opening of internal cavities during the dissolution process resulted in losses of
533 phytC found in these locations, which is expected when phytoliths are subject to rapid oxidation.
534 Conversely, phytC in the silica network is homogeneously distributed at the micrometric scale,
535 and is less accessible to oxidation. These two pools of phytC may account for the heterogeneity
536 of phytC accessibility to oxidation.

537

538 **4.2. Rebuttals to possible arguments against the SOM derived-C contribution to phytC** 539 **hypothesis**

540 Our experiments and dataset allow the rejection of several hypotheses for the
541 “anomalously” old ^{14}C ages for phytC. First, bias due to exogenous C contamination during the
542 phytolith extractions performed simultaneously by several laboratories and artifacts of errors in
543 background corrections are highly unlikely. In these cases the ^{14}C offsets would trend in a single
544 direction, rather than being both positive and negative (Figures 2b and 4). In addition, aliquots of
545 SiO_2 blank and fossil phytoliths (MSG70) reference material yielded ^{14}C values in close
546 agreement with the expected results, giving no indication of the presence of unusual
547 contaminants. Second, natural- or spectrometer-produced anomalous $\delta^{13}\text{C}$ shifts of phytC were
548 not observed here (Figures 3 and 5) nor elsewhere (Santos et al., 2010, Santos et al., 2012b,
549 Sullivan and Parr, 2013). Third, contributions of soil respired CO_2 to mature plant tissue (and
550 phytC) were also negligible (section 2.2.3). Fourth, phytC ^{14}C results were not biased by organic
551 matter residues, as the efficiency of the phytolith extraction protocols was fully checked by
552 SEM-EDS analyses (e.g. acceptance threshold of $\text{C}:\text{Si} \leq 0.1$ of 30 frames or more) (Corbineau et
553 al., 2013), a method superior to microscopic evaluation alone (Figures S1 and S2) (Kameník et
554 al., 2013, Santos et al., 2012a). Moreover, our extracts were consistently reproducible regarding
555 phytC yields across all labs involved (Tables S1-S3) and thermal decomposability properties

556 (Figure 6). Since it has been established that plants do not photosynthesize all carbon found
557 within their tissues (details in section 4.5), the uptake of SOM-derived C via the root system and
558 its allocation to phytC is the only plausible explanation for the phytC ^{14}C offsets.

559

560 **4.3. Implications for the use of phytC as a proxy of plant C**

561 Since plants (and more specifically phytoliths) contain a broad continuum of C with a
562 complex mixture of chemical compounds of different turnover times as evidenced here (Figures
563 2, 4, and 6), we believe that insufficient to excessive oxidations can result in wild moves in
564 phytC ^{14}C dates from thousands, to hundreds, to back to thousands years old (Figure 7).

565 While pure surface phytoliths produced from a less aggressive protocol (e.g. 1a) may
566 minimize ^{14}C offsets to some degree, two factors remain that may explain the anomalous
567 thousands of years old age of phytC indicated in the literature (Wilding, 1967, Kelly et al., 1991,
568 McClaran and Umlauf, 2000, Santos et al., 2010, Santos et al., 2012a, Sullivan and Parr, 2013,
569 and recently, Piperno 2015 and Santos et al. 2016). The first factor is the incomplete removal
570 from phytolith concentrates of refractory SOM residues, either extraneous in the case of litter
571 and soil samples or from the plant tissue itself. The accumulation effect of small quantities of
572 residual recalcitrant (and somewhat older) SOM derived-C from concentrates due to incomplete
573 digestion (Figure 7), which can be detected via C:Si peaks with SEM-EDS (Corbineau et al.
574 2013), may be undetected under natural light microscopy. For instance, Santos et al. (2010)
575 reported phytC ^{14}C age offsets of 2.3 to 8.5 kyrs BP on phytolith concentrates extracted from
576 living grasses using conventional digestion protocols, such as Kelly et al. (1991). Later, OM
577 remnants in association with those anomalous ^{14}C results were detected by SEM-EDS on
578 phytolith concentrates (Figure 2 in Santos et al. 2012a), thus demonstrating that even very small
579 amounts of surface C were enough to bias the phytC ^{14}C results. Attempts to reproduce the
580 atmospheric $^{14}\text{CO}_2$ bomb-peak in phytC from bamboo litter and mature leaves subjected to
581 microwave digestions, also yielded offsets of several hundreds to 3.5 kyrs (Santos et al., 2012b,
582 Sullivan and Parr, 2013). Similarly, a set of post-bomb Neotropical plant phytolith extracts
583 produced by two protocols yielded phytC ^{14}C ages that were highly inaccurate, e.g. phytC ^{14}C
584 offsets ranging from several decades to 4.4 kyrs (Santos et al. 2016). In those cases, preferential
585 bias due to post-depositional occlusion of SOM was unlikely. All phytolith extracts analyzed
586 were obtained from living or close to living vegetation, undergoing different extraction

587 procedures coupled with optical microscope analyses (for purity evaluations). Cumulative effects
588 of OM remnants on phytoliths would also explain the higher phytC yields (Kelly et al., 1991, Li
589 et al., 2014, Parr and Sullivan, 2005, Santos et al., 2010, Song et al., 2014). The second factor is
590 the increasing relative proportion of old SOM-derived C in phytC when phytolith extraction
591 aggressiveness is high enough to remove the phytC fraction most sensitive to oxidation (e.g. the
592 labile-accessible C fraction termed ‘protocol 2’ in Figure 7). Once carbon partitioning takes
593 place via either further chemical extractions or increased combustion temperatures, phytC
594 concentrations tend to drop followed by increased ^{14}C offsets to thousands of years old (Yin et
595 al., 2014 and the present work).

596 Since the range of old SOM-derived C content in phytC left by a given protocol can be
597 large (Figure 2), and can vary in association to the abundances of C fractions within the
598 substrates and their respective ^{14}C signatures (Figure 4), any attempt to apply a systematic
599 correction to obtain a phytC Fm^{14}C signature derived solely from photosynthesis is likely to fail.
600 We can also assume that when grasses are forced to reach greater rooting depths (Sivandran and
601 Bras, 2012) than the ones sampled here, where the proportion of intrinsic-older organic
602 compounds is likely to rise (Teller et al. 2003, Torn et al. 2009, Kleber, 2010, Petsch et al.,
603 2001), old SOM-derived C in phytC and its Fm^{14}C depletions would also increase. Furthermore,
604 by themselves the ^{14}C signatures of phytC pools with competing ^{14}C ages (recent SOM-derived
605 C vs present-day atmospheric $^{14}\text{CO}_2$) are insufficient to distinguish them. Therefore, the old soil-
606 C to phytC contributions found here in association with the ^{14}C signatures of phytoliths extracted
607 from living grasses are likely to be only a very small fraction of the total SOM contribution to
608 phytC, as discussed earlier.

609 Further work is still needed to assess the full impact of SOM (e.g., the different fractions
610 of labile vs. recalcitrant carbon; Han et al., 2007) to the phytC pool. At natural conditions the
611 presence of SOM-derived C in phytC may bias the $\delta^{13}\text{C}$ signature to a lesser extent if the SOM
612 and the plants of origin have similar photosynthetic pathways (C_3 or C_4). The bias may however
613 be significant if they are not. The $\delta^{13}\text{C}$ signature of SOM can be hard to assess, especially in the
614 case of phytoliths extracted from sedimentary archives. Thus, we suggest that the use of ^{14}C and
615 $\delta^{13}\text{C}$ signatures of phytC as a dating tool or as a proxy of plant or atmospheric CO_2 signatures
616 should be reappraised in the light of the present findings.

617

618 **4.4. Implications for long-term atmospheric CO₂ biosequestration**

619 The evidence for a SOM-derived C contribution to phytC decreases the putative
620 effectiveness of grasslands and crops to sequester atmospheric CO₂ for two reasons. Besides
621 negatively affecting phytolith C storage capacity, our findings most importantly invalidate phytC
622 accumulation rates estimated from direct ¹⁴C dating of soil phytoliths (Parr and Sullivan, 2005).
623 In addition, other issues may also come into play. For instance, the phytolith biosequestration
624 hypothesis is based essentially on the following premises. First, high phytC concentrations are
625 required. Values of 1.5-3% d.wt. have been quantified (e.g. Li *et al.*, 2013, Parr and Sullivan,
626 2011, Parr *et al.*, 2010). These values are more than 10 times higher than the concentrations
627 recently measured by others (<0.1% d.wt. [Santos *et al.*, 2010]). Differences in the efficiency of
628 phytolith extraction protocols (Kameník *et al.*, 2013), combined with the lack of proper control
629 (blanks) and reproducibility of results (Corbineau *et al.*, 2013) may have contributed to these
630 high phytC concentrations. Second, a soil phytolith stability factor of 70 to 90% based on a few
631 ¹⁴C measurements of soil phytoliths (e.g. Parr and Sullivan, 2005) has been estimated and widely
632 used (Li *et al.*, 2014) regardless of soil type. These high percentage estimates differ from those of
633 biogenic Si fluxes, based on Si pool measurements in tropical soil-plant systems. For instance,
634 according to Alexandre *et al.* (2011) investigating two soil/plant systems in intertropical areas,
635 only 10% of phytoliths produced annually are in fact preserved for extended periods, the
636 remaining 90% being rapidly dissolved due to weathering (Oleschko *et al.*, 2004). These
637 proportions would reasonably depend on environmental conditions such as activity of elements
638 (Si, Al, Fe, H+) in soil solution, morphology of phytoliths (and thus vegetation type), elemental
639 concentration of phytoliths (and thus soil type).

640 Only as an exercise, we used the highest phytC yield measured in the frame of the present
641 study (0.3% of phytoliths) coupled with the 10% phytolith stability factor estimated from
642 Alexandre *et al.* (2011), to recalculate a global grassland phytC-sink. We obtain a value of 4.1
643 $\times 10^4$ tC yr⁻¹, which is roughly one hundred times lower than the 3.7×10^6 tC yr⁻¹ value reported
644 elsewhere (Song *et al.*, 2014 and references therein). This amount is insignificant when
645 compared to the 2.6×10^9 tC yr⁻¹ estimate for the land C sink (I.P.C.C. Staff, 2007), or to the
646 0.4×10^9 tC yr⁻¹ global mean long term soil C accumulation rate (Schlesinger, 1990). This

647 suggests that previous conclusions on the importance of developing silica accumulator crops for
648 increasing atmospheric C sequestration should be reconsidered.

649

650 **4.5. Implications for our understanding of soil C pools mobilization.**

651 Our findings have important implications for our understanding of the mobilization of
652 soil C pools. Several studies have shown that terrestrial plant roots can uptake soil dissolved
653 inorganic carbon (DIC). DIC can be transported directly by the transpiration stream or fixed in
654 mycorrhizal and root tissues and subsequently translocated in the form of amino acid (Gioseffi et
655 al., 2012, Rasmussen et al., 2010, Talbot and Treseder, 2010). DIC can represent 1 to 3% of
656 total leaf-fixed CO₂ (Ford et al., 2007, Ubierna et al., 2009). However, as DIC is expected to be
657 in equilibrium with soil CO₂ respired from autotrophic and heterotrophic sources, its ¹⁴C
658 signature should reflect an average of SOM ¹⁴C signatures, close to contemporary. Assuming soil
659 DIC as the soil end-member in Figure 2, the phytC samples from ambient CO₂ experiments
660 would plot along mixing lines with lower slopes than the actual ones. The ¹⁴C age of several
661 thousand years systematically measured for the most resistant phytC, rather suggests that an
662 older SOM fraction supplies the SOM-derived C absorbed by the roots, up-taken and transported
663 to the stem and leaves tissues.

664 The fact that roots can also acquire soil C in a molecular form has been previously
665 inferred from the detection in roots, stems and shoots of polycyclic aromatic hydrocarbons
666 (PAH) (Gao et al., 2010, Yu et al., 2013), and soil amino acids (AA) (Paungfoo-Lonhienne et al.,
667 2008, Warren, 2012, Whiteside et al., 2012, Whiteside et al., 2009). Although reported PAH
668 concentrations were three orders of magnitude below phytC concentrations (e.g. 10⁻⁹ g/g vs. 10⁻⁶
669 g/g, assuming 0.1% d.wt. for both phytolith concentration in plants and phytC content in
670 phytoliths), AAs make up several tenths of % of the plant nitrogen requirements (Lipson and
671 Näsholm, 2001). Arbuscular mycorrhizal fungi, which colonize 70% of plant families (Talbot
672 and Treseder, 2010, Treseder and Turner, 2007) are probably at the base of the transfer of
673 molecular C from the rhizosphere to the roots, although intact protein has also been shown to
674 enter root cells without the help of mycorrhizae, most likely via endocytosis (Paungfoo-
675 Lonhienne et al., 2008). At lower scales, AA transporters were shown to confer the ability of
676 plants to absorb molecular C from the soil solution (Lipson and Näsholm, 2001, Tegeder, 2012).
677 Root acquisition of humic substances (active and passive) and its positive effect on plant nutrient

678 uptake has been also reported (Trevisan et al., 2010). The incorporation of below-ground
679 physical, chemical and biological processes in the rhizosphere (e.g. microbial priming effect or
680 nitrogen (N) and C cycles interactions) have also been proposed (Heimann and Reichstein, 2008
681 and references therein). The results of the present study go a step further by demonstrating that
682 part of the soil molecular C absorbed by roots is several thousand years old. Recent studies also
683 show that old, supposedly poorly accessible SOM (Kleber, 2010, Petsch et al., 2001, Schmidt et
684 al., 2011), can be decomposed by organisms or catalytic enzymes (Dungait et al., 2012, Marín-
685 Spiotta et al., 2014). Common sources of dissolved Si for plants are clay minerals and
686 amorphous silicates (allophane, imogolite). Due to their small size, high surface functional
687 groups, area, and porosity, these minerals stabilize SOM either by adsorption onto their surface
688 or by aggregation (Basile-Doelsch et al., 2007, Jones and Singh, 2014, Kögel-Knabner et al.,
689 2010). Further studies are needed to investigate whether dissolution of Si-bearing forms during
690 active uptake of Si (Ma et al., 2006) may also promote old SOM mobilization, ready to be
691 chelated with Si, absorbed by the roots and translocated to the stems and leaves.

692

693 **5. Conclusion**

694 Although photosynthesis is the main source of C in plant tissue, we have demonstrated
695 here that grass biosilica (phytoliths) occlude SOM-derived C that can be several thousand years
696 old, debunking the common assumption of phytC photosynthetic carbon exclusivity. This finding
697 suggests causes for previous anomalously older phytC ^{14}C ages found in the literature. Moreover,
698 the fact that phytC is not uniquely constituted of photosynthetic C limits the usefulness of phytC
699 either as a dating tool or as a significant sink of atmospheric CO_2 . Revised estimates of
700 atmospheric CO_2 biosequestration by phytoliths led to values that are insignificant compared to
701 the total land C or soil C sinks. All in all, by demonstrating that old SOM-derived C is accessible
702 to roots and builds-up in plant biosilica, this study constitutes a basis to further investigate the
703 mechanism and amplitude of old SOM recycling by roots for a better understanding of the C
704 cycle at the soil/plant interface.

705

706 **Author Contributions:** G.M.S. conceived the study. G.M.S., A.A., P.E.R., and R.C. designed
707 the experiments and conceived the strategies for phytolith extraction and purity analyses.
708 G.M.S., P.E.R., A.A., A.H., R.C. and H.M. performed the experiments and contributed to
709 analysis tools. F.B. and L.C. provided bulk tissue and soil samples from T. Durum FACE.
710 G.M.S., A.A., and P.E.R. interpreted the data and wrote the paper. All authors discussed the
711 results and implications, and commented on the manuscript.

712

713 **Acknowledgements:** The authors gratefully acknowledge the support of the U.S.
714 National Science Foundation (DEB-1144888 to GMS), the French FIR 2010 (Aix-Marseille
715 Université), ECCOREV 2011, AIR Archéométrie 2011(CNRS) and Labex OT-Med 2013. PER
716 wishes to thank J.A. Mason (University of Wisconsin-Madison) and the National Lacustrine
717 Core Facility (University of Minnesota) for lab space usage. GMS thanks M.J. Ottman, B.
718 Kimball, S.W. Leavitt, E. Pendall, P. Pinter, G. Hendrey, H. L. Cho and R. Rauschkolb for
719 providing the archived Maricopa FACE samples. Financial support provided by the Durum
720 experiment via the "Fondazione in rete per la ricerca agroalimentare" with the AGER program:
721 agroalimentare e ricerca is gratefully acknowledged. We thank J. Southon for help with the ¹⁴C-
722 AMS analyses, and C. Czimczik and M. Lupasco for technical support with the CO₂ flux
723 measurements, help in interpreting the data, and suggestions and comments on an early version
724 of this paper. We would like to thank X. Xu for the stable isotope analysis and technical support
725 for CO₂-air cryogenic extraction, and Q. Lin and the Laboratory for Electron and X-ray
726 Instrumentation (LEXI) at UC Irvine for access to lab space and assistance with X-ray analytical
727 techniques. We also thank S. Fahrni for providing the inorganic fertilizer used in the control
728 planter, and K. Gallagher for her efforts on the estimates of percent carbon of some amendments.
729 A.A. thanks J. Balesdent (CEREGE) for helpful discussion on root absorption of molecular C.
730 The authors also wish to extend their thanks to the Editor Dr. Roland Bol and the three
731 anonymous reviewers for the constructive comments.

732

733 **References**

734

735 Alexandre, A., Bouvet, M., Abbadie, L. The role of savannas in the terrestrial Si cycle: A case-
736 study from Lamto, Ivory Coast. *Global and Planetary Change*, 78, 162-169, 2011.

737 Alexandre, A., Basile-Doelsch, I., Delhaye, T., Borshneck, D., Mazur, J.C., Reyerson, P., Santos,
738 G.M. New highlights of phytolith structure and occluded carbon location: 3-D X-ray
739 microscopy and NanoSIMS results. *Biogeosciences*, 12, 863-873, 2015.

740 Badeck, F.W., Rizza, F., Maré, C., Cattivelli, A., Zaldei, F., Miglietta, F. Durum wheat growth
741 under elevated CO₂: first results of a FACE experiment. In: *Proceedings of the XVI*
742 *National Congress of Agrometeorology: Agrometeorology for Environmental and Food*
743 *Security*. pp Page. Bologna, Pàtron Editore, 2012.

744 Bae, M-S., Schauer, J.J., Deminter, J.T., Turner, J.R., Smith, D., Cary, R.A. Validation of a
745 semi-continuous instrument for elemental carbon and organic carbon using a thermal-
746 optical method. *Atmospheric Environment*, 38, 2885-2893, 2004.

747 Basile-Doelsch, I., Amundson, R., Stone, W.E.E., Borschneck, D., Bottero, J. Y., Moustier, S.,
748 Masin, F., Colin, F. Mineral control of carbon pools in a volcanic soil horizon.
749 *Geoderma*, 137, 477-489, 2007.

750 Bauer, P., Elbaum, R., Weiss, I.M. Calcium and silicon mineralization in land plants: Transport,
751 structure and function. *Plant Science*, 180, 746-756, 2011.

752 Beverly, R., Beaumont, W., Tauz, D., Ormsby, K., Von Reden, K., Santos, G.M., Southon, J.R.
753 The Keck Carbon Cycle AMS Laboratory, University of California Irvine: status report.
754 *Radiocarbon*, 52, 301-309, 2010.

755 Carter, J.A. Atmospheric carbon isotope signatures in phytolith-occluded carbon. *Quaternary*
756 *International*, 193, 20-29, 2009.

757 Cheng, P., Zhou, W., Wang, H., Lu, X., Du, H. ¹⁴C dating of soil organic carbon (SOC) in loess-
758 paleosol using sequential pyrolysis and accelerator mass spectrometry (AMS).
759 *Radiocarbon*, 55, 563-570, 2013.

760 Corbineau, R., Reyerson, P.E., Alexandre, A., Santos, G.M. Towards producing pure phytolith
761 concentrates from plants that are suitable for carbon isotopic analysis. *Review of*
762 *palaeobotany and palynology*, 197, 179-185, 2013.

763 Crespin, J., Alexandre, A., Sylvestre, F., Sonzogni, C., Pailles, C., Garreta, V. IR laser extraction
764 technique applied to oxygen isotope analysis of small biogenic silica samples. *Annals of*
765 *Chemistry*, 80, 2372-2378, 2008.

766 Czimzik, C.I., Trumbore, S.E., Carbone, M.S., Winston, G.C. Changing sources of soil
767 respiration with time since fire in a boreal forest *Global Change Biology*, 12, 957-971,
768 2006.

769 Deer, W.A., Howie, R.A., Zussman, J. An introduction to the rock-forming minerals, Essex,
770 Longman Scientific and Technical, 2nd edn., Longman Scientific and Technical, Essex,
771 1992, 696 pp.

772 Dungait, J. A., Hopkins, D. W., Gregory, A. S., Whitmore, A. P. Soil organic matter turnover is
773 governed by accessibility not recalcitrance. *Global Change Biology*, 18, 1781-1796,
774 2012.

775 Fernandez, A., Santos, G. M., Williams, E. K., Pendergraft, M. A., Vetter, L., Rosenheim, B. E.
776 Blank corrections for ramped pyrolysis radiocarbon dating of sedimentary and soil
777 organic carbon. *Analytical Chemistry*, 86, 12085-12092, 2014.

778 Ford, C. R., Wurzbarger, N., Hendrick, R. L., Teskey, R. O. Soil DIC uptake and fixation in
779 *Pinus taeda* seedlings and its C contribution to plant tissues and ectomycorrhizal fungi.
780 *Tree physiology*, 27, 375-383, 2007.

781 Gao, Y., Cheng, Z., Ling, W., & Huang, J. Arbuscular mycorrhizal fungal hyphae contribute to
782 the uptake of polycyclic aromatic hydrocarbons by plant roots. *Bioresource Technology*,
783 101, 6895-6901, 2010.

784 Geis, J.W. Biogenic silica in selected species of deciduous angiosperms. *Soil Science*, 116, 113-
785 130, 1973.

786 Gioseffi, E., Neergaard, A. D., Schjørring, J. K. Interactions between uptake of amino acids and
787 inorganic nitrogen in wheat plants. *Biogeosciences*, 9, 1509-1518, 2012.

788 Han, Y., Cao, J., An, Z., Chow, J. C., Watson, J. G., Jin, Z., Fung, K., Liu, S. Evaluation of the
789 thermal/optical reflectance method for quantification of elemental carbon in sediments.
790 *Chemosphere*, 69, 526-533, 2007.

791 Harvey, O. R., Kuo, L. J., Zimmerman, A. R., Louchouart, P., Amonette, J. E., & Herbert, B. E.
792 An Index-Based Approach to Assessing Recalcitrance and Soil Carbon Sequestration

793 Potential of Engineered Black Carbons (Biochars). *Environmental science & technology*,
794 46, 1415-1421, 2012.

795 Heimann, M. and Reichstein, M. Terrestrial ecosystem carbon dynamics and climate feedbacks.
796 *Nature*, 451, 289-292, 2008.

797 Hibberd, J.M. and Quick, W.P. Characteristics of C₄ photosynthesis in stems and petioles of C₃
798 flowering plants. *Nature*, 415, 451-454, 2002.

799 I.P.C.C. *Climate Change 2007: Synthesis Report. Contribution of Working Groups I, II and III to*
800 *the Fourth Assessment Report of the Intergovernmental Panel on Climate Change*,
801 Geneva, Switzerland, 2007.

802 Jones, E. and Singh, B. Organo-mineral interactions in contrasting soils under natural vegetation.
803 *Frontiers in Environmental Science*, 2, 2, 2014.

804 Kameník, J., Mizera, J., Řanda, Z. Chemical composition of plant silica phytoliths.
805 *Environmental Chemistry Letters*, 11, 189-195, 2013.

806 Kelly, E. F., Amundson, R. G., Marino, B. D., Deniro, M. J. Stable isotope ratios of carbon in
807 phytoliths as a quantitative method of monitoring vegetation and climate change.
808 *Quaternary Research*, 35, 222-233, 1991.

809 Kleber, M. What is recalcitrant soil organic matter? *Environmental Chemistry*, 7, 320-332, 2010.

810 Kögel-Knabner, I., Amelung, W., Cao, Z., Fiedler, S., Frenzel, P., Jahn, R., Kalbitz, K., Kölbl,
811 A., Schloter, M. (2010) Biogeochemistry of paddy soils. *Geoderma*, 157, 1-14, 2010.

812 Leavitt, S.W. Carbon isotope dynamics of CO₂-enriched FACE cotton and soils. *Agricultural and*
813 *Forest Meteorology*, 70, 87-101, 1994.

814 Leavitt, S. W., Pendall, E., Paul, E. A., Brooks, T., Kimball, B. A., Pinter, P. J., Johnson, B.,
815 Matthias, A., Wall, G.W., LaMorte, R. L. Stable-carbon isotopes and soil organic carbon
816 in wheat under CO₂ enrichment. *New Phytologist*, 150, 305-314, 2001.

817 Levin, I. Twenty Years of Atmospheric CO₂ Observations At Schauinsland Station, Germany.
818 *Radiocarbon*, 39, 205-218, 1997.

819 Levin, I., Kromer, B., Hammer, S. Atmospheric $\Delta^{14}\text{CO}_2$ trend in Western European background
820 air from 2000 to 2012. *Tellus B*, 65, 2013.

821 Li, B., Song, Z., Li, Z., Wang, H., Gui, R., Song, R. Phylogenetic variation of phytolith carbon
822 sequestration in bamboos. *Sci. Rep.*, 4, 2014.

823 Li, Z., Song, Z., Parr, J. F., Wang, H. Occluded C in rice phytoliths: implications to
824 biogeochemical carbon sequestration. *Plant and Soil*, 370, 615-623, 2013.

825 Lipson, D. and Näsholm, T. The unexpected versatility of plants: organic nitrogen use and
826 availability in terrestrial ecosystems. *Oecologia*, 128, 305-316, 2001.

827 Ma, J. F., Tamai, K., Yamaji, N., Mitani, N., Konishi, S., Katsuhara, M., Ishiguro, M., Murata,
828 Y., Yano, M. A silicon transporter in rice. *Nature*, 44, 688-691, 2006.

829 Marín-Spiotta, E., Gruley, K. E., Crawford, J., Atkinson, E. E., Miesel, J. R., Greene, S.,
830 Cardona-Correa, C., Spencer, R. G. M. Paradigm shifts in soil organic matter research
831 affect interpretations of aquatic carbon cycling: transcending disciplinary and ecosystem
832 boundaries. *Biogeochemistry*, 117, 279-297, 2014.

833 Mcclaran, M.P. and Umlauf, M. Desert Grassland Dynamics Estimated from Carbon Isotopes in
834 Grass Phytoliths and Soil Organic Matter. *Journal of Vegetation Science*, 11, 71-76,
835 2000.

836 Mcinerney, F.A., Strömberg, C.A.E., White, J.C. The Neogene transition from C3 to C4
837 grasslands in North America: stable isotope ratios of fossil phytoliths. *Paleobiology*, 37,
838 23-49, 2011.

839 Nardi, S., Pizzeghello, D., Muscolo, A., Vianello, A. Physiological effects of humic substances
840 on higher plants. *Soil Biology & Biochemistry*, 34, 1527-1536, 2002.

841 Oleschko, K., Parrot, J. F., Ronquillo, G., Shoba, S., Stoops, G., Marcelino, V. Weathering:
842 toward a fractal quantifying. *Mathematical Geology*, 36, 607-627, 2004.

843 Ottman, M. J., Kimball, B. A., Pinter, P. J., Wall, G. W., Vanderlip, R. L., Leavitt, S. W.,
844 LaMorte, R.L., Matthias, A.D., Brooks, T. J. Elevated CO₂ increases sorghum biomass
845 under drought conditions. *New Phytologist*, 150, 261-273, 2001.

846 Parr, J.F. and Sullivan, L.A. Soil carbon sequestration in phytoliths. *Soil Biology and*
847 *Biochemistry*, 37, 117-124, 2005.

848 Parr, J. and Sullivan, L. Phytolith occluded carbon and silica variability in wheat cultivars. *Plant*
849 *and Soil*, 342, 165-171, 2011.

850 Parr, J., Sullivan, L., Quirk, R. Sugarcane phytoliths: Encapsulation and sequestration of a long-
851 lived carbon fraction. *Sugar Tech*, 11, 17-21, 2009.

852 Parr, J., Sullivan, L., Chen, B., Zheng, W. Carbon bio-sequestration within the phytoliths of
853 economic bamboo species. *Global Change Biology*, 16, 2661-2667, 2010.

854 Paungfoo-Lonhienne, C., Lonhienne, T. G., Rentsch, D., Robinson, N., Christie, M., Webb, R. I.,
855 Gamage, H.K. Carroll, B.J., Schenk, P.M., Schmidt, S. Plants can use protein as a
856 nitrogen source without assistance from other organisms. *Proceedings of the National*
857 *Academy of Sciences*, 105, 4524-4529, 2008.

858 Pausch, J. and Kuzyakov, Y. Photoassimilate allocation and dynamics of hotspots in roots
859 visualized by ^{14}C phosphor imaging. *Journal of Plant Nutrition and Soil Science*, 174,
860 12-19, 2011.

861 Petsch, S. T., Eglinton, T. I., & Edwards, K. J. ^{14}C -dead living biomass: evidence for microbial
862 assimilation of ancient organic carbon during shale weathering. *Science*, 292, 1127-1131,
863 2001.

864 Piperno, D.R. *Phytoliths: a comprehensive guide for archaeologists and paleoecologists*,
865 Lanham, MD, AltaMira Press, 304pp, 2006.

866 Piperno, D.R. Phytolith radiocarbon dating in archaeological and paleoecological research: a
867 case study of phytoliths from modern Neotropical plants and a review of the previous
868 dating evidence. *J. Archaeol. Sci.* 2015, (<http://dx.doi.org/10.1016/j.jas.2015.06.002>), *in*
869 *press*.

870 Piperno, D.R. and Stothert, K.E. Phytolith evidence for early Holocene Cucurbita domestication
871 in southwest Ecuador. *Science*, 299, 1054-1057, 2003.

872 Plante, A.F., Pernes, M., Chenu, C. Changes in clay-associated organic matter quality in a C
873 depletion sequence as measured by differential thermal analyses. *Geoderma*, 129, 186-
874 199, 2005.

875 Plante, A.F., Fernández, J.M., Haddix, M.L., Steinweg, J.M., Conant, R.T. Biological, chemical
876 and thermal indices of soil organic matter stability in four grassland soils. *Soil Biology &*
877 *Biochemistry* 43(5), 1051–8, 2011.

878 Plante, A.F., Beaupré, S.R., Roberts, M.L. and Baisden, T. Distribution of Radiocarbon Ages in
879 Soil Organic Matter by Thermal Fractionation. *Radiocarbon*, 55(2–3), 1077-1083, 2013.

880 Raich, J.W. and Sclesinger, W.H. The global carbon dioxide flux in soil respiration and its
881 relationship to vegetation and climate. *Tellus B*, 44, 81-99, 1992.

882 Rasmussen, J., Sauheitl, L., Eriksen, J., Kuzyakov, Y. Plant uptake of dual-labeled organic N
883 biased by inorganic C uptake: Results of a triple labeling study. *Soil Biology and*
884 *Biochemistry*, 42, 524-527, 2010.

885 Raven, J.A. Cycling Silicon: The Role of Accumulation in Plants. *New Phytologist*, 158, 419-
886 421, 2003.

887 Rosenheim, B. E., Santoro, J. A., Gunter, M., Domack, E. W. Improving Antarctic sediment C-
888 ¹⁴C dating using ramped pyrolysis: an example from the Hugo Island Trough.
889 *Radiocarbon*, 55, 115-126, 2013.

890 Runge, F. The opal phytolith inventory of soils in central Africa - Quantities, shapes,
891 classification, and spectra. *Review of palaeobotany and palynology*, 107, 23-53, 1999.

892 Santos, G.M. and Ormsby, K. Behavioral variability in ABA chemical pretreatment close to the
893 ¹⁴C age limit. *Radiocarbon*, 55, 534-544, 2013.

894 Santos, G. M., Southon, J. R., Druffel-Rodriguez, K. C., Griffin, S., Mazon, M. Magnesium
895 perchlorate as an alternative water trap in AMS graphite sample preparation: A report on
896 sample preparation at KCCAMS at the University of California, Irvine. *Radiocarbon*, 46,
897 165-173, 2004.

898 Santos, G. M., Moore, R. B., Southon, J. R., Griffin, S., Hinger, E., Zhang, D. Ultra small-mass
899 ¹⁴C-AMS sample preparation and analysis at the KCCAMS Facility. *Nuclear*
900 *Instruments and Methods in Physics Research B*, 259, 293-302, 2007.

901 Santos, G. M., Alexandre, A., Coe, H. H., Reyerson, P. E., Southon, J. R., De Carvalho, C. N.
902 The phytolith ¹⁴C puzzle: a tale of background determinations and accuracy tests.
903 *Radiocarbon*, 52, 113-128, 2010.

904 Santos, G. M., Alexandre, A., Southon, J. R., Treseder, K. K., Corbineau, R., Reyerson, P. E.
905 Possible source of ancient carbon in phytolith concentrates from harvested grasses.
906 *Biogeosciences*, 9, 1873-1884, 2012a.

907 Santos, G. M., Southon, J. R., Alexandre, A., Corbineau, R., Reyerson, P. E. Interactive
908 comment on "Comment on: "Possible source of ancient carbon in phytolith concentrates
909 from harvested grasses" by G. M. Santos et al. (2012)" by L. A. Sullivan and J. F. Parr.
910 *Biogeosciences Discussions*, 9, C6114-C6124, 2012b.

911 Santos, G.M., Alexandre, A., Prior, C.A. (2016) From radiocarbon analysis to interpretation: A
912 comment on "Phytolith Radiocarbon Dating in Archaeological and Paleocological
913 Research: A Case Study of Phytoliths from Modern Neotropical Plants and a Review of
914 the Previous Dating Evidence", *Journal of Archaeological Science* (2016), doi:

915 10.1016/j.jas.2015.06.002.” by Dolores R. Piperno, Journal of Archaeological Science,
916 (doi: 10.1016/j.jas.2015.11.012), *in press*.

917 Schlesinger, W.H. Evidence from chronosequence studies for a low carbon-storage potential of
918 soils. *Nature*, 348, 232-234, 1990.

919 Schmidt, M. W., Torn, M. S., Abiven, S., Dittmar, T., Guggenberger, G., Janssens, I. A., Kleber,
920 M., Trumbore, S. E. Persistence of soil organic matter as an ecosystem property. *Nature*,
921 478, 49-56, 2011.

922 Schrumpf, M., Kaiser, K., Guggenberger, G., Persson, T., Kögel-Knabner, I., & Schulze, E. D.
923 Storage and stability of organic carbon in soils as related to depth, occlusion within
924 aggregates, and attachment to minerals. *Biogeosciences*, 10, 1675-1691, 2013.

925 Sivandran, G. and Bras, R.L. Identifying the optimal spatially and temporally invariant root
926 distribution for a semiarid environment. *Water Resources Research*, 48, 12, 2012.

927 Smith, F.A. and White, J.W.C. Modern calibration of phytolith carbon isotope signatures for
928 C3/C4 paleograssland reconstruction. *Palaeogeography, Palaeoclimatology,*
929 *Palaeoecology*, 207, 277-304, 2004.

930 Song, Z., Parr, J. F., Guo, F. Potential of global cropland phytolith carbon sink from optimization
931 of cropping system and fertilization. *PLOS One*, 8, e73747, 2013.

932 Song, Z., Wang, H., Strong, P. J., Guo, F. Phytolith carbon sequestration in China's croplands.
933 *European Journal of Agronomy*, 53, 10-15, 2014.

934 Stuiver, M and Polach, H. Reporting of ¹⁴C data. *Radiocarbon*, 19, 355-363, 1977.

935 Sullivan, L.A. and Parr, J.F. Comment on "Possible source of ancient carbon in phytolith
936 concentrates from harvested grasses" by G. M. Santos et al. (2012). *Biogeosciences*, 10,
937 977-980, 2013.

938 Suttie, J. M., Reynolds, S. G. Batello, C. *Grasslands of the World* (FAO, 2005), 2005.

939 Talbot, J.M. and Treseder, K.K. Controls of mycorrhizal uptake of organic nitrogen.
940 *Pedobiologia*, 53, 169-179, 2010.

941 Tegeder, M. Transporters for amino acids in plant cells: some functions and many unknowns.
942 *Current Opinion in Plant Biology*, 15, 315-321, 2012.

943 Telles, E.C.C., Camargo, P.B., Martinelli, L.A., Trumbore, S.E., Costa, E.S., Santos, J., Higuchi,
944 N., Oliveira Jr., R.C. Influence of soil texture on carbon dynamics and storage potential

945 in tropical forest soils of Amazonia. *Global Biogeochem. Cycles* 17 (2), 1040, 2003
946 (<http://dx.doi.org/10.1029/2002GB001953>)

947 Toma, Y., Clifton-Brown, J., Sugiyama, S., Nakaboh, M., Hatano, R., Fernández, F. G., Stewart,
948 J.R., Nishiwaki, A., Yamada, T. Soil carbon stocks and carbon sequestration rates in
949 seminatural grassland in Aso region, Kumamoto, Southern Japan. *Global Change*
950 *Biology*, 19, 1676-1687, 2013.

951 Torn, M.S., Swanston, C.W., Castanha, C., Trumbore, S.E. Storage and turnover of organic
952 matter in soil. In: Senesi, N., Xing, B., Huang, P.M. (Eds.), *Biophysicochemical*
953 *Processes Involving Natural Nonliving Organic Matter in Environmental Systems.*
954 *International. Union of Pure and Applied Chemistry (IUPAC)*, New York, NY, pp. 219-
955 272, 2009.

956 Treseder, K.K. and Turner, K.M. Glomalin in ecosystems. *Soil Science Society of America*
957 *Journal*, 71, 1257-1266, 2007.

958 Trevisan, S., Francioso, O., Quaggiotti, S., Nardi, S. Humic substances biological activity at the
959 plant-soil interface. *Plant Signaling & Behavior*, 5, 635-643, 2010.

960 Ubierna, N., Marshall, J. D., & Cernusak, L. A. A new method to measure carbon isotope
961 composition of CO₂ respired by trees: stem CO₂ equilibration. *Functional Ecology*, 23,
962 1050-1058, 2009.

963 Warren, C.R. Post-uptake metabolism affects quantification of amino acid uptake. *New*
964 *Phytologist*, 193, 522–531, 2012

965 Webb, E.A. and Longstaffe, F.J. The oxygen isotopic compositions of silica phytoliths and plant
966 water in grasses: Implications for the study of paleoclimate. *Geochimica et*
967 *Cosmochimica Acta*, 64, 767-780, 2000.

968 Webb, E.A. and Longstaffe, F.J. Limitations on the climatic and ecological signals provided by
969 the $\delta^{13}\text{C}$ values of phytoliths from a C₄ North American prairie grass. *Geochimica et*
970 *Cosmochimica Acta*, 74, 3041-3050, 2010.

971 Whiteside, M. D., Digman, M. A., Gratton, E., & Treseder, K. K. Organic nitrogen uptake by
972 arbuscular mycorrhizal fungi in a boreal forest. *Soil Biology and Biochemistry*, 55, 7-13,
973 2012.

974 Whiteside, M. D., Treseder, K. K., & Atsatt, P. R. The brighter side of soils: quantum dots track
975 organic nitrogen through fungi and plants. *Ecology*, 2009.

976 Wichern, F., Andreeva, D., Joergensen, R. G., Kuzyakov, Y. Stem labeling results in different
977 patterns of ^{14}C rhizorespiration and ^{15}N distribution in plants compared to natural
978 assimilation pathways. *Journal of Plant Nutrition and Soil Science*, 174, 732-741, 2011.

979 Wilding, L.P. Radiocarbon dating of biogenetic opal. *Science*, 156, 66-67, 1967.

980 Wu, Y., Yang, Y., Wang, H., Wang, C. The effects of chemical composition and distribution on
981 the preservation of phytolith morphology. *Applied Physics A*, 114, 503-507, 2014.

982 Xu, X., Trumbore, S. E., Zheng, S., Southon, J. R., McDuffee, K. E., Luttgen, M., Liu, J. C.
983 Modifying a sealed tube zinc reduction method for preparation of AMS graphite targets:
984 Reducing background and attaining high precision. *Nuclear Instruments and Methods in*
985 *Physics Research Section B: Beam Interactions with Materials and Atoms*, 259, 320-329,
986 2007.

987 Yin, J., Yang, X., & Zheng, Y. Influence of increasing combustion temperature on the AMS ^{14}C
988 dating of modern crop phytoliths. *Sci. Rep.*, 4. 2014

989 Yu, W., Kuang, S., Zhao, L. Uptake, accumulation and translocation of polycyclic aromatic
990 hydrocarbons by winter wheat cultured on oily sludge-amended soil. *Chinese Journal of*
991 *Geochemistry*, 32, 295-302, 2013.

992

Table 1: Below-ground experiment. Details of substrate amendments, their carbon content, radiocarbon values (as Fm14C and ^{14}C age) and C isotopic signatures.

Name	Major Contents	%C (mass) ^a	Fm ¹⁴ C	$\pm 1\sigma$	¹⁴ C age	$\pm 1\sigma$	$\delta^{13}\text{C}$ (‰)	$\pm 1\sigma$
Miracle Gro® (MG)	<i>Sphagnum Moss, Perlite, Compost, NH₄NO₃, (NH₄)₃PO₄, Ca₃(PO₄)₂, K₂SO₄</i>	49.5 (n=2)	1.0849	0.0028	-650 ^b	25	-26.1	0.1
			1.0123	0.0028	-95 ^b	25	-25	0.1
Greensand (GS)	<i>Glauconite with organic and inorganic detritus, MnO₂, SiO₂</i>	0.10 ^c	0.1591 (n=2)	0.0016	14765	78	-24.3(OC; n=4) -12.6(bulk)	0.1
Ionic Grow (IG)	<i>Ca(NO₃)₂, KNO₃, H₃PO₄, HNO₃, K₂SO₄</i>	0.8	0.0374 (n=2)	0.0101	26550	2192	-26.4	0.1
Earth juice (EJ)	<i>Kelp meal, MgSO₄ borax, CoSO₄, FeSO₄, MnSO₄, Na₂MoO₄, ZnSO₄</i>	15.44 (n=2)	0.4991 (n=3)	0.0013	5583	24	-24.1 (n=2)	0.2
Fossil Fuel (FF)	<i>Humic acids (from leonardite or lignite coal)</i>	33.04 (n=2)	0.0055	0.0003	43340	1700	-26.2 (n=2)	0.2
Inorganic in-house fertilizer (IF)^d	<i>NaH₂PO₄, MgSO₄, Ca(NO₃)₂, KNO₃</i>	-----	-----	-----	-----	-----	-----	-----
Silica Blast (SB)^d	<i>Na₂SiO₃, K₂SiO₃</i>	-----	-----	-----	-----	-----	-----	-----

^aTotal percent carbon was determined by manometric measurements of CO₂ after combustion of solids. Those values are estimates only, as it does not take in account volatile organic C losses during the drying procedure of the amendments as solutions; ^bnegative ¹⁴C ages are associated with material that fixed C during the post-nuclear testing period (e.g. Post-AD 1950 to present); ^cGS %C is based on its total C amount by d.wt., with 0.06% of it constituted of organic matter detritus with the remaining C pool from marine carbonates. %C estimates of independent fractions were based on stable isotopic measurements of bulk and HCl treated (OC fraction) subsamples (section 2.2.2). Nevertheless, the FmC ¹⁴C values of the organic C and bulk fractions are similar, and are shown here as an average value. The $\delta^{13}\text{C}$ values of both fractions are shown as reference; ^dattempts to produce CO₂ from solids (upon freeze-dry) confirmed the absence of C in those amendments, and therefore those are not shown.

Table 2: Below-ground experiment. Planters' major features: substrates and amendments, living plant appearance, biomass by d.wt. and phytolith yields. All nutrients and fertilizers were administered in aqueous solutions, except for MG. In bold: main amendment.

	Planters					
	A	B	C	D	E	F
Substrate	MG	GS	Baked Sand	Baked Sand	Baked Sand	Baked Sand
Amendments	In MG	In GS, IG^a	IG^a	EJ, IF^b	FF, IF^b	IF^b
Silica Provider	In MG	In GS	SB	SB	SB	SB
Appearance	Dark green	Dark green	Dark green	Green	Yellowish green	Green
Biomass (g)	98.57	79.09	89.24	86.67	54.78	53.37
Phytolith yield^c	0.12	0.78	0.83	0.83	1.77	1.35

^aIG has a very low %C. Therefore, its C contribution to planters B and C after dilution into solution (e.g. ~ 0.02 grams of C per feeding) was found to be very small, a conclusion supported by isotopic analyses (Table S3); ^bIF (which does not contain measurable amounts of C) was added to those planters to supply micronutrients to support plant growth; ^cas % of dry leaf and stem biomass combined.

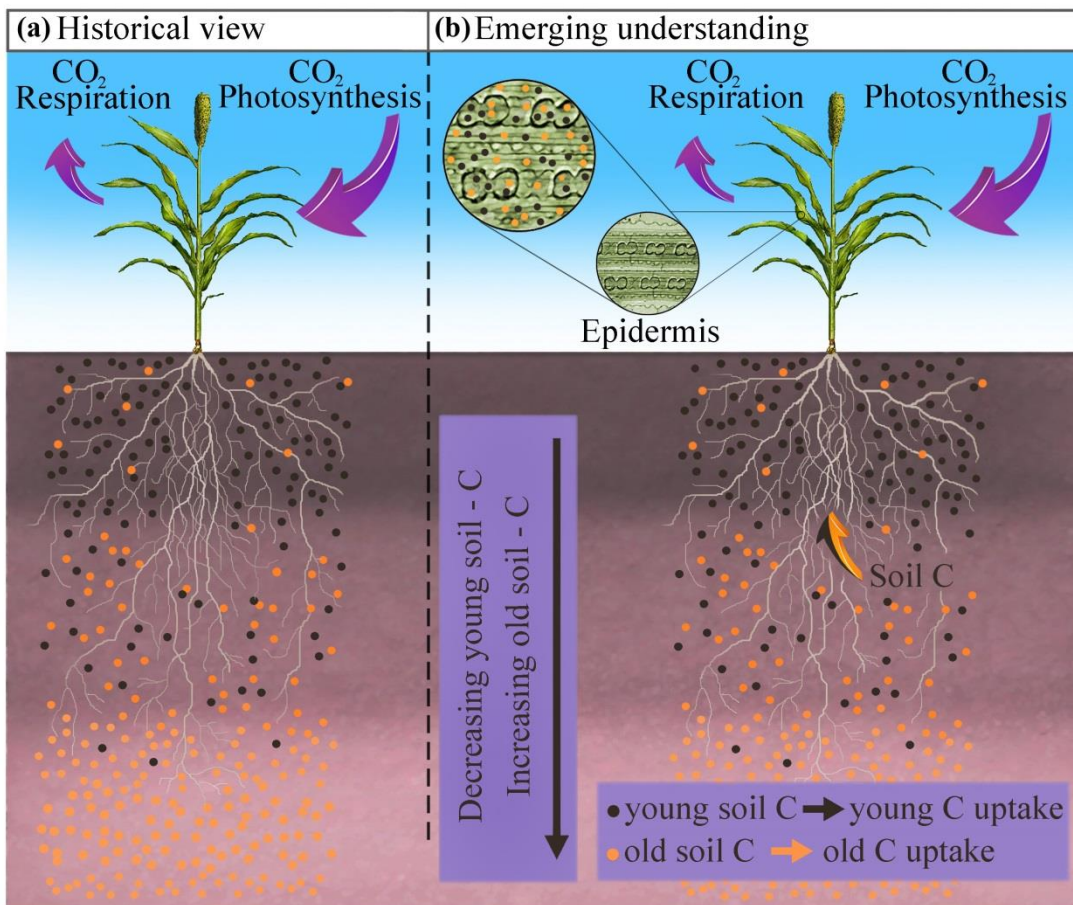


Fig. 1: Sketch of a) the conventional hypothesis of plant C occlusion during silica precipitation based solely on atmospheric CO_2 as a source, and b) the emerging hypothesis of a dual origin (atmospheric CO_2 and SOM) for plant C (and phytC). Young and old soil C distributed in leaf epidermis (green tissue) and phytoliths (illustrated by the bilobate type shape outlined in black) are represented by black and orange dots, respectively, in the microscope diagram.

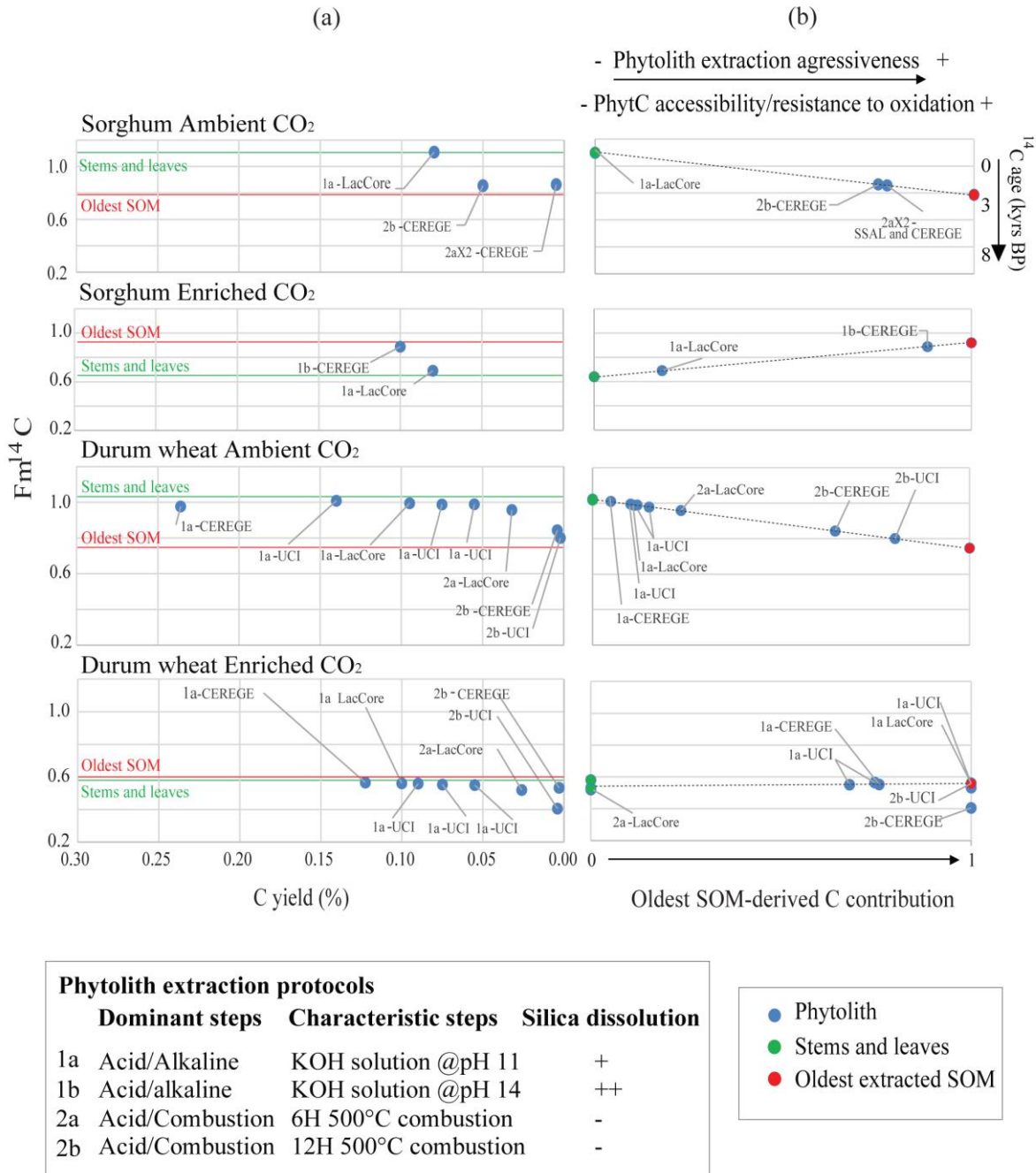


Fig. 2: Above ground C manipulation procedure. a) Averaged $Fm^{14}C$ values versus averaged phytC yields (or concentration in % of phytoliths). Constant solid lines correspond to the averaged $Fm^{14}C$ values obtained for stems and leaves (SL) of origin and the oldest extracted SOM fraction. b) Oldest SOM-derived C contribution to phytC calculated using the mixing equation (eq. 1) presented in the text expressing the ^{14}C signature of phytC as the result of mixing between the C derived from plant photosynthesis and the C derived from the oldest

extracted SOM fraction. Phytolith samples are labeled according to the extraction protocol (1a, 1b, 2a, 2b described in caption and in the text) used and the laboratory of extraction (UCI, CEREGE, LacCore and SSAL).

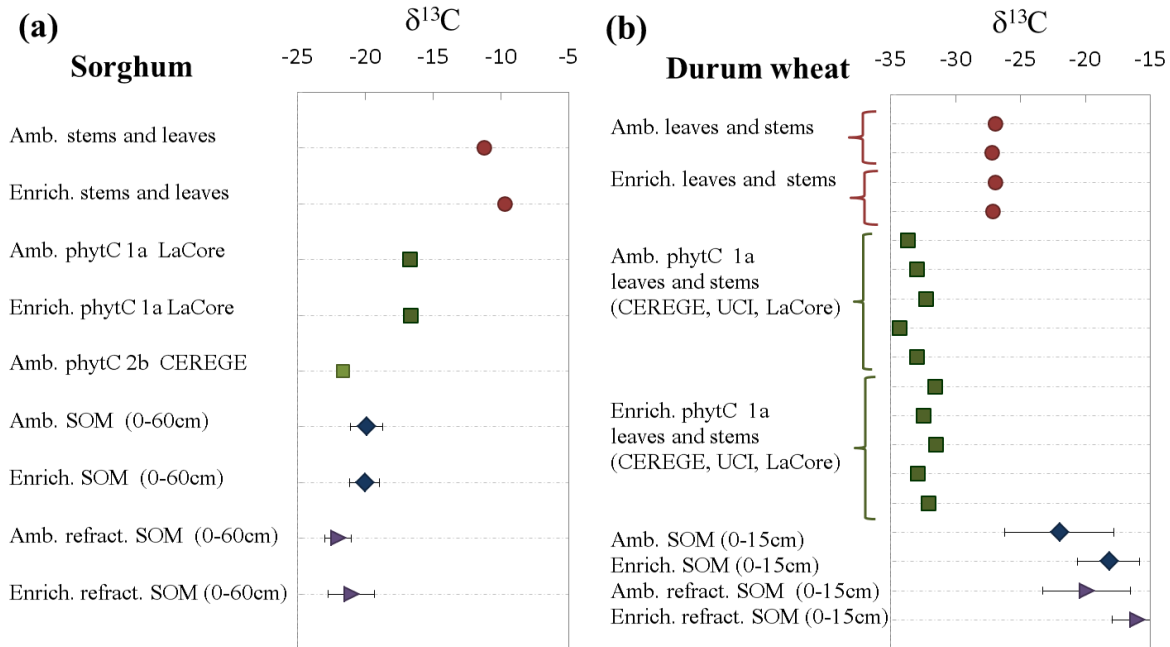


Fig. 3. Above-ground C manipulation experiment. $\delta^{13}\text{C}$ values of stems and leaves, phytC, and soil SOM fractions obtained for A) sorghum and B) durum wheat experiments. To facilitate comparisons between groups, samples from ambient and enriched CO_2 plots are plotted next to each other. Values are reported as per mil (‰) related to PDB. Results of the bulk and refractory SOM fractions were averaged; consequently results and uncertainties indicate multiple data points. Individual results are shown in Tables S1 and S2.

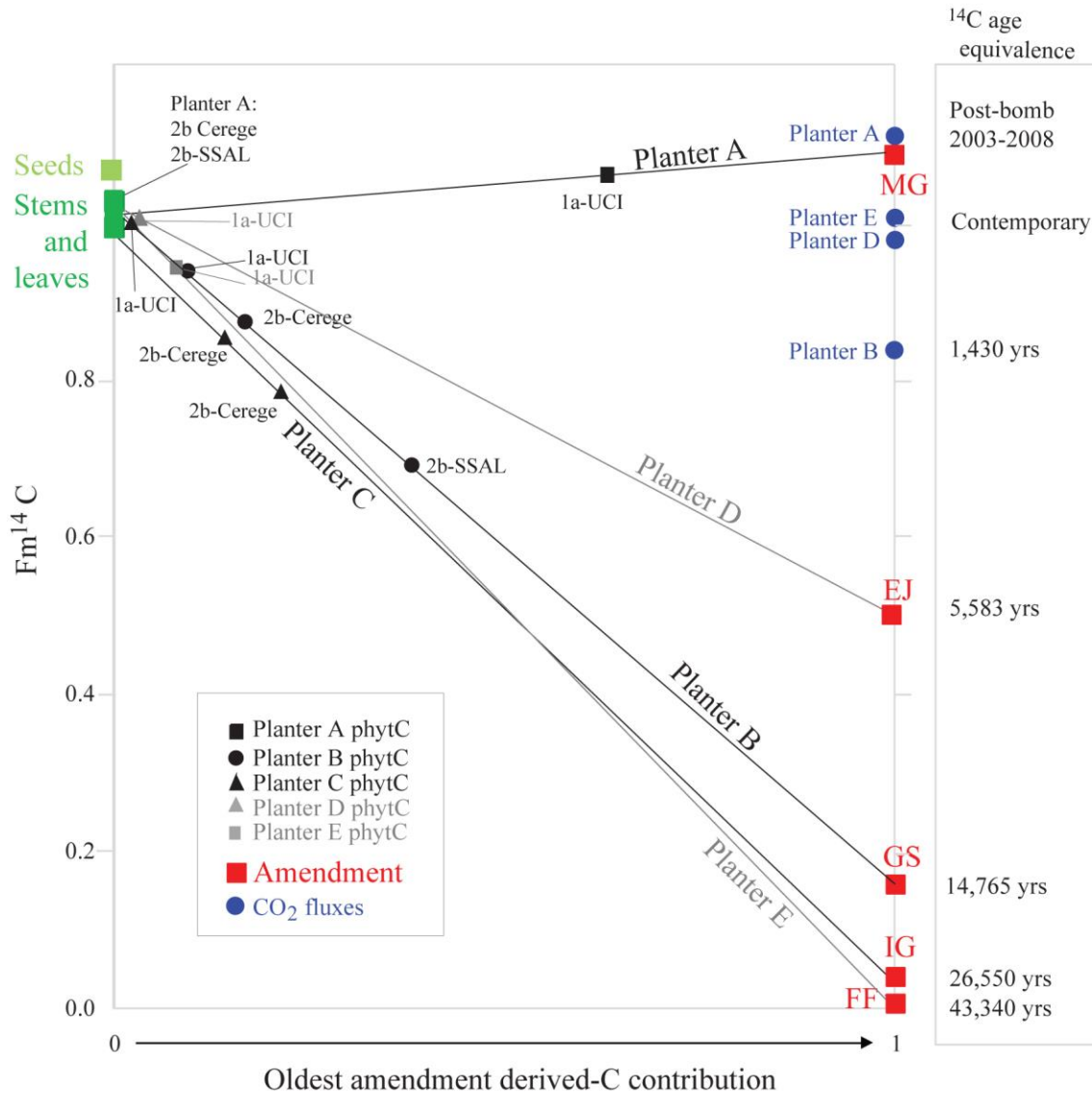


Fig. 4. Below ground C manipulation procedure: Oldest amendment-derived C contribution to phytC calculated using the mixing equation (eq. 1) presented in the text expressing the ^{14}C signature of phytC as the result of mixing between C derived from plant photosynthesis (seeds, stems and leaves represented by the green squares) and C derived from the oldest amendment (MG, EJ, GS, IG, FF defined in table 1 and represented by the red squares). Phytolith samples are labeled according to the phytolith extraction protocol used (1a and 2b) and the laboratory of extraction (UCI, CEREGE and SSAL). Selected age benchmarks from substrate amendments and soil CO_2 fluxes are shown for reference on the right axis.

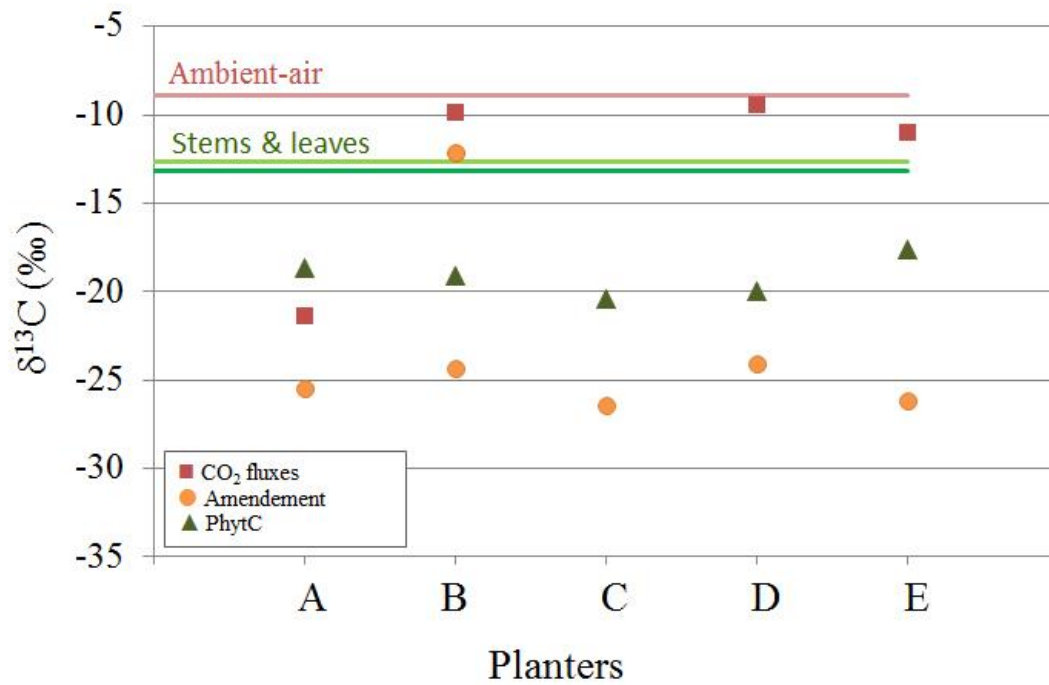


Fig. 5. Below-ground C manipulation experiment. $\delta^{13}\text{C}$ values of the respired CO₂, stems and leaves, amendments and phytC for the five planters enriched in organic carbon nutrients (A-E). Values are reported as per mil (‰) related to PDB, and individual symbols represent single results as reported in Table S3. For planter B we report two values, its OC fraction (-24.3‰) and its bulk fraction (-12.1‰ – a mixture of OC and inorganic carbon) (Table 1). Constant solid lines correspond to the average $\delta^{13}\text{C}$ values of ambient-air CO₂ and bulk plant tissues.

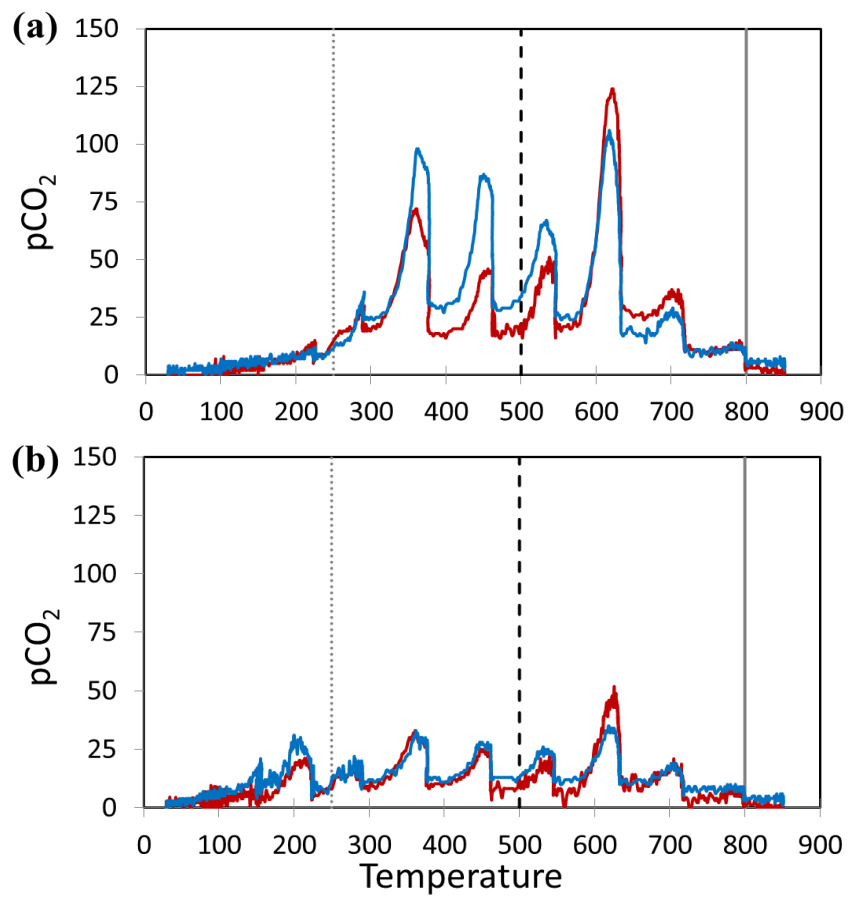


Fig. 6: Thermograms ($n=2$; blue and red lines) of phytoliths obtained from a) durum wheat leaves, phytoliths extracted following protocol 1a (Table S2), and b) soil phytoliths MSG70 extracted using a conventional protocol adapted to soil and sediment materials. Peaks are artifacts of the 100°C temperature-step increments. Vertical lines indicate main temperature thresholds, as explained in text.

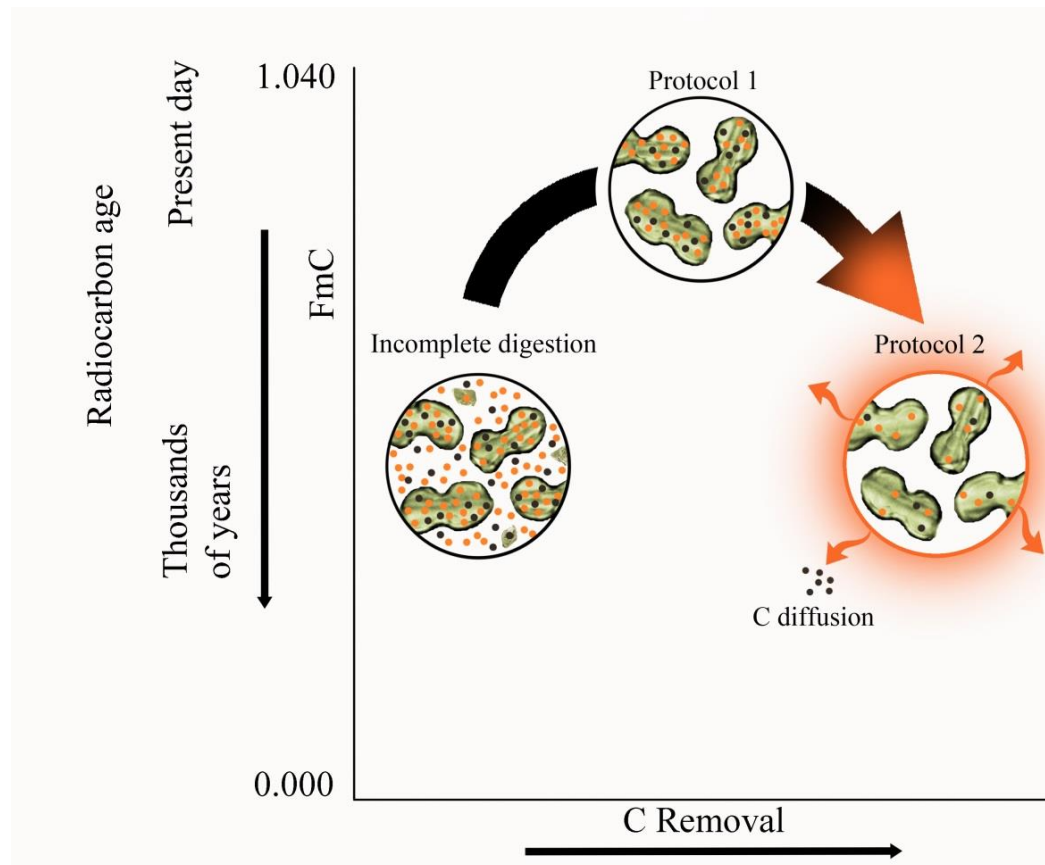


Fig. 7: Conceptualization of the impact of phytolith extraction aggressiveness and C removal on ^{14}C age of phytoliths. Incomplete digestion leads to an accumulation of old SOM residues on phytolith extract surfaces. Protocol 1 removes all surface OM and better preserves the dual source phytC signature. Protocol 2 removes all surface OM and labile (intrinsically young) phytC from inside the silica network. For illustration purposes, young and old C are represented by black and orange dots, respectively (cf Figure 1b).